NASA Technical Memorandum 81799

Mass Loss of a TEOS-Coated, Reinforced Carbon-Carbon Composite Subjected to a Simulated Shuttle Entry Environment

C. W. Stroud and Donald R. Rummler

JULY 1980

NASA

NASA Technical Memorandum 81799

Mass Loss of a TEOS-Coated, Reinforced Carbon-Carbon Composite Subjected to a Simulated Shuttle Entry Environment

C. W. Stroud and Donald R. Rummler
Langley Research Center
Hampton, Virginia

National Aeronautics
and Space Administration

**Scientific and Technical
Information Office**

1980

SUMMARY

Reinforced carbon-carbon (RCC) is used for the leading edges of the Space Shuttle. The baseline material is coated with tetraethyl orthosilicate (TEOS) for additional oxidation resistance and is then designated as TEOS-coated RCC. Most previous testing of this material to determine its mass-loss characteristics consisted of alternate exposures to temperature, oxygen partial pressure, and stress cycles to simulate the Shuttle operational environment. In contrast, the present investigation included simultaneous application of load, temperature, and oxygen partial pressure to simulate the Shuttle entry environment more closely. The mass-loss characteristics of TEOS-coated RCC specimens were determined for conditions which simulated the entry environment expected at the lug attachment area of the leading edge. Maximum specimen temperature was 900 K (1160° F). Specimens were exposed for up to 80 simulated missions.

Stress levels up to 6.8 MPa (980 psi) did not significantly affect the mass-loss characteristics of the TEOS-coated RCC material. Mass loss was correlated with the bulk density of the specimens.

INTRODUCTION

The thermal protection system for the leading-edge areas of the Space Shuttle is constructed of a reinforced carbon-carbon material (RCC). RCC is a laminated carbon-carbon substrate with an oxidation-resistant coating. In spite of the coating, RCC was found to undergo moderate oxidation at temperatures and oxygen partial pressures typical of Shuttle entry. Consequently, methods for further improvements in oxidation protection for RCC were investigated (refs. 1 to 5). These efforts concentrated on the development of a second coating that could be applied over the baseline coating. A second coating that was lightweight and had superior oxidation resistance in certain ranges of temperature and oxygen partial pressure was developed in 1976 by Vought Corporation. Tetraethyl orthosilicate (TEOS) is applied to the coated part using a vacuum impregnation process, and the material with this second coating is designated as TEOS-coated RCC.

The first objective of the present investigation was to determine whether externally applied stress had a significant effect on the mass loss of TEOS-coated RCC material. The second objective was to obtain mass-loss data for TEOS-coated RCC under conditions of simultaneous application of temperatures, oxygen partial pressures, and stresses encountered at the lug attachment area of the Shuttle wing leading edge during entry. Both objectives were achieved by subjecting TEOS-coated RCC specimens to an environment which simulated flight-by-flight entry conditions in the lug attachment area of the Shuttle wing leading edge. The lug area was selected because both stress and mass loss were high in this region. On the Shuttle, the lug area is protected from external flow and heated by conduction and radiation from the heated

leading-edge surface. The wing location simulated in these tests was at 55 percent half-span where extensive thermostructural analyses had been previously performed. Temperatures in this area, where the leading edge attaches to the wing substructure, do not exceed 900 K (1160° F), but the stresses are 6.8 MPa (980 psi) at the peak temperature. A complete factorial experiment was carried out with stress at two levels (zero and full operational stress). The factorial experiment was designed to achieve the first objective. A required subset of the factorial experiment generated the data necessary to achieve the second objective.

SYMBOLS

The units used for the physical quantities defined below are given in both the International System of Units (SI) (ref. 6) and in U.S. Customary Units. The measurements and calculations were made in U.S. Customary Units.

A_p	calculated planform area, m^2 (ft^2)
B	mass-loss constant
d	diameter, m (ft)
E_i	activation energy, J/mole (cal/mole)
$F_\alpha(v_1,v_2)$	ratio of variances of two independent random samples
K_i	mass-loss rate constant
ℓ	length, m (ft)
m	mass loss, kg/m^2 (lb/ft^2)
m_L	accumulated mass loss, kg/m^2 (lb/ft^2)
$\dot{m}$	mass-loss rate, kg/m^2-s $(lb/ft^2$-sec$)$
n	pressure exponent
P	pressure, Pa (atm)
R	gas constant, 8.3143 J/mole-K (1.987 cal/mole-°R)
r_i	shoulder radius, m (ft)
T	temperature, K (°R)
t_i	thickness, m (ft)

t_w weighted thickness, m (ft)

V_b bulk volume, m^3 (ft^3)

v_1 degrees of freedom for the sample variance of the numerator

v_2 degrees of freedom for the sample variance of the denominator

w_i width, m (ft)

ρ bulk density, kg/m^3 (lb/ft^3)

Subscripts:

i integer

N number of missions

α upper probability level

TEST SPECIMENS

Nine RCC mass-loss specimens were cut from a sheet of 33-ply material according to the specimen layout shown in figure 1. The sheet material is a laminate made from a phenolic prepregged, square-weave graphite-cloth fabric pyrolyzed to the carbon state. The pyrolyzed substrate was subjected to three furfuryl alcohol impregnations, each followed by pyrolysis to improve density and strength. After being cut from the sheet, the specimens were machined to size. Next, the baseline oxidation-resistant coating was applied to each specimen by packing the composite in a powder composed by weight of 60 percent silicon carbide, 10 percent aluminum oxide, and 30 percent silicon. The packed specimens were then heated to a high temperature in an inert atmosphere. The TEOS coating was subsequently applied to each specimen using a vacuum impregnation process. The impregnated specimens were then cured at 363 K (195° F). The impregnation process was repeated five times before the final curing process at 590 K (600° F) for 3.5 hours. The coating produced by this process is a microamorphous silica. Photographs of a typical as-received specimen are shown in figure 2.

The nominal dimensions of the TEOS-coated RCC specimens are shown in figure 3. The method used to determine actual specimen dimensions is given in appendix A. Table I presents the results of measurements to determine the actual dimensions of each specimen. Table II presents other physical characteristics of the TEOS-coated RCC specimens: as-received mass, mass after drying, calculated bulk volume, bulk density, calculated surface area, effective cross-sectional area, and weighted thickness (as defined in appendix A).

EQUIPMENT AND PROCEDURES

Multiparameter Test System

All tests in this study were performed in a multiparameter test system at the Langley Research Center. A block diagram and a photograph of this system are shown in figure 4. The system consists of three vacuum furnaces, analog controls, and computer complex. Each vacuum furnace has the capability of independently loading six thin-sheet tensile specimens simultaneously. Cylindrical clamshell heating elements surround all six loading locations in each vacuum furnace. The heated zone of the furnaces is 150 mm (6 in.) in diameter and 300 mm (12 in.) long. Each of the three vacuum chambers can be controlled continuously over a pressure range of 1.33 mPa (10^{-5} torr) to 101.3 kPa (760 torr). The three control parameters - specimen load, temperature, and chamber pressure - are each controlled by the analog closed-loop servo system. Thus, when the full capacity of the system is used, temperature and pressure histories can be controlled independently for each of the 3 groups of 6 specimens, and loads can be controlled independently for each of the 18 specimens under test. A process-control computer provides the control signals for each vacuum chamber for the desired parameter history and also monitors system responses such as temperature, specimen load, and chamber pressure. Digital-to-analog (D/A) and analog-to-digital (A/D) converters provide communication links between the computer and vacuum furnaces. Twenty-five temperatures, six loads, and one pressure from each stand can be monitored by the computer.

For the current test series, only one vacuum chamber was used. The chamber was modified to test three relatively thick (10 mm (0.39 in.)) specimens simultaneously. The modification was necessary to provide clearance between the thick specimens and the heating elements. The configuration of the modified loading system is shown schematically in figure 5. During a test, the three specimens consisted of a control specimen, which indirectly controlled the temperature, and two test specimens (the latter in chamber locations designated as A and B). Also shown is the inlet air distribution manifold. This manifold directs air onto the test specimen surface to assure purging of that area of combustion products. A vacuum pump draws gas through the carbon dioxide monitoring tube to a carbon dioxide analyzer (appendix B), thus verifying that an oxidizing atmosphere is present at all times. Figure 6 gives a detailed sketch of the load train and shows the location of thermocouples in a graphite calibration specimen which was used to determine temperature distributions during system calibration.

Testing Procedures

The nominal test specimen temperature, stress level, and chamber air pressure histories are presented in figure 7. The histories in figure 7 were generated using the values listed in table III with linear interpolation between points of temperature and stress, and logarithmic interpolation between

points of pressure. These histories indicate environmental conditions at the lug attachment area of the leading edge of the Shuttle during reentry. The desired tolerances for the three controlled variables with respect to nominal profiles were as follows:

Temperature:
± 16.7 K ($\pm 30^{\circ}$ F)

Air pressure:
± 267 Pa for $0 < P \leq 13.3$ kPa (± 2 torr for $0 < P \leq 100$ torr)
± 666 Pa for 13.3 kPa $< P \leq 101.3$ kPa (± 5 torr for 100 torr $< P \leq 760$ torr)

Stress:
± 5 percent or ± 170 kPa (± 25 psi), whichever is larger

An additional requirement of the Shuttle program was that the dew point of the inlet air be less than 230 K (-48° F) to simulate the relatively dry air encountered during reentry and minimize the catalytic effects of moisture on the oxidation of carbon.

The desired tolerance in temperature could not be achieved in the multi-parameter simulator because the heavy ceramic end fittings and the shielding of the ends of the specimens from radiation caused temperature gradients along the length of the specimen. These gradients exceeded the desired temperature tolerance. (See appendix C for details.) Because the desired temperature tolerance could not be achieved, another criterion was sought to judge the quality of simulation. The criterion selected was based upon the mass loss calculated using a mass-loss prediction equation developed by Vought Corporation (eq. (D1), appendix D). The calculated mass loss using temperatures and pressures obtained during calibration mission cycles is summarized in appendix C. Calibration procedures demonstrated that -

1. The calculated mass losses for all points on the specimen are well within the nominal range associated with the desired control tolerances for temperature and air pressure.

2. The reproducibility from one mission cycle to the next is excellent.

Facility calibration indicated that sample location in the furnace could be a significant source of experimental variability. For this reason, sample location was randomized as much as possible by changing the furnace location (A or B) of the loaded specimen each time a new set of specimens was tested. Since two specimens were tested at a time, one was loaded to the mission profile and the other kept under a constant small stress of less than 170 kPa (25 psi) (hereinafter referred to as the no-load condition). The specimens were tested in pairs as follows:

Test series	Specimen number[a]	Load condition	Furnace location
I (50 missions)	3	Load	A
	5	No load	B
II (80 missions)	1	No load	A
	9	Load	B
III (50 missions)	6	Load	A
	7	No load	B
IV (75 missions)	4	No load	A
	8	Load	B

[a]See figure 1.

To minimize contamination, the specimens were handled with clean plastic gloves. The order in which the test specimens were removed from the test chamber, weighed, and photographed was alternated each time the specimens were removed (five-mission intervals). The specimens were stored in a desiccator except when they were in the test chamber or when they were being photographed and weighed. This procedure minimized the transport of oxygen to the interior of the specimen by moisture absorption.

The simulated missions were monitored with an on-line plotter which displayed the differences between the command and the response of the three controlled parameters. An on-line printer provided a hard copy of parameter values at six-second intervals. Data were recorded on tape at six-second intervals and used for subsequent analysis.

RESULTS AND DISCUSSION

Mass-Loss Data

The mass-loss data for eight specimens are tabulated in table IV (specimen 2 was used for temperature control). The mass loss per unit surface area is listed after five-mission test intervals. The mass loss was obtained as follows:

$$\text{Mass loss} = \frac{\text{Initial dry weight} - \text{Current weight}}{\text{Surface area}} \tag{1}$$

All values of mass loss in the following discussion are based on mass loss per unit surface area. Specimens 3, 5, 6, and 7 were tested for 50 missions. Testing was halted at this point to obtain residual strength data after 50 missions. Specimens 1 and 9 and specimens 4 and 8 were tested in pairs until the

mass loss of one of the pair exceeded 488 g/m^2 (0.100 lb/ft^2). A plot of the mass loss of each specimen is shown in figure 8. All specimens exhibit a monotonically increasing mass-loss rate. In order to amplify any trends that might be common to all specimens, plots of the average mass loss per mission during each five-mission cycle block are shown in figure 9. The mass loss per mission tends to drop during the 6- to 10-mission interval, then to increase in subsequent missions. This behavior may indicate that part of the mass loss occurring during the first five missions is due to a volatile component in either the material or the coating that was not driven off by the drying procedure. This trend is quite obvious in all four loaded specimens. Of the unloaded specimens, only specimen 7 clearly shows the drop in rate at 10 missions. Specimens 4 and 5 show slight decreases in rate at 10 missions.

Photographs of specimen 1 after 80 missions are shown in figure 10. This specimen was typical of all specimens tested. Visual examinations of all specimens before and after testing revealed no apparent changes due to environmental exposure.

Analysis of Variance of Mass Loss

One of the major objectives of this study was to determine whether the simultaneous application of load, temperature, and oxygen partial pressure to the TEOS-coated RCC material caused higher mass loss than when only temperature and pressure were applied. In addition to the load parameter, an additional variable of furnace location was inherent in the test results. Two furnace locations, A and B, were used to reduce the testing time, and as indicated in table IV, mass loss was affected by furnace location. Thus, two levels of load and two furnace locations were considered. To resolve these effects, the testing was carried out as a complete factorial experiment with replication.

The mass-loss results after 50 missions are shown in the following table:

Factor 1: furnace location	Factor 2: load or no load	Replication 1	Replication 2
		Mass loss, g/m^2	Mass loss, g/m^2
A	Load	356.81	266.73
B	No load	298.52	228.16
A	No load	276.69	308.92
B	Load	254.08	219.37
Total		1186.10	1023.18

The following analysis of variance (in accordance with ref. 7) was generated from these results:

Source of variation	Degrees of freedom	Sum of squares	Mean square	F
Main effects:				
Location	1	5 461.07	5 461.07	2.8540
Load	1	292.02	292.02	.1520
Interaction	1	1 038.63	1 038.63	.5428
Error	4	7 653.70	1 913.43	
Total	7	14 181.29		

The values of F show that both the main effects and the interaction are insignificant at the 95-percent confidence level. That is, none of these values exceed the $F_{.05}(1,4)$ value of 7.71. These results indicate that neither load nor location had a statistically significant effect in these tests; however, a comparison of the F values shows that furnace location was the more important factor in explaining mass-loss variability.

Comparison of Data With Empirical Predictions

A comparison of the measured mass loss with the mass loss predicted by an empirical equation is shown in figure 11. This empirical equation was developed by Vought Corporation and is defined in appendix D, equation (D1). The nominal mission parameters were used to calculate the predicted mass loss plotted in figure 11. The mass loss predicted by the equation is seen to lie well below the experimental data envelope. Further calculations were made using the actual temperature and pressure recorded when specimens 1 and 9 were tested for 80 missions. Figure 12 shows the results of these calculations compared with the experimental mass loss of specimens 1 and 9 and the average mass loss of all specimens. The average mass loss for all the specimens tested is very close to the average mass loss of specimens 1 and 9. After 80 missions, the predicted mass loss is only 66 percent of the average experimental mass loss. Throughout the test series, the predicted mass loss was substantially lower than the average mass loss obtained during testing. Because of this large discrepancy between predicted and experimental results, Vought Corporation modified the prediction equation. The modified equation (appendix D, eq. (D2)) was used to recalculate the expected mass loss. The results of these calculations are shown in figure 13. The mass loss predicted by the modified equation is in good agreement with average experimental mass losses throughout the mission range. These calculations used actual chamber parameters for specimens 1 and 9. Similar calculations were made using mission parameters of specimens 4 and 8 with comparable results. Based on these comparisons, the modified equation appears to adequately predict the observed mass losses.

Effects of RCC Bulk Density on Mass Loss

Results presented previously show that neither load nor furnace location was a statistically significant factor in explaining the mass-loss differences among specimens. The one unique feature of each specimen was the location in the panel from which each specimen was cut. Figure 14 shows the panel location of each specimen and a plot of calculated bulk density (appendix A) for each specimen. Specimen 9 was cut from the panel at 90° to the remaining specimens and might be expected to behave differently. The one apparent trend is a higher bulk density in the specimens cut from the edges of the original panel. In figure 15, the mass loss after 50 missions is plotted as a function of calculated initial bulk density. A trend is immediately apparent. The greater the initial bulk density, the smaller the mass loss. Specimen 7 does not follow this trend. It was so far from the other data that it was considered an outlier and eliminated from further consideration. A linear least-squares curve fit was made of the mass-loss data, and the following equation was obtained:

$$m_{50} = 9321.5 - 5598\rho \tag{2}$$

where ρ is the initial bulk density in grams per centimeter cubed, and m_{50} is the predicted mass loss after 50 missions, in grams per meter squared. Normalizing mass loss with respect to the 50-mission correlation, yields

$$\text{Normalized mass loss} = \frac{m_N}{m_{50}} \tag{3}$$

where m_N is the measured mass loss after N missions (in g/m^2), and m_{50} is the predicted mass loss after 50 missions (in g/m^2). Values of normalized mass loss can exceed 1, since some specimens were tested for more than 50 missions. The mass loss, normalized to the density-correlated mass loss after 50 missions, is plotted (fig. 16) as a function of mission cycles. The normalized data range over a narrow band with specimens 1 and 8 on the upper and lower extremes, respectively. The bulk density correlation reduced the scatter significantly. Before application of the density correlation, the data had a ratio of maximum mass loss to minimum mass loss of 1.63 (see fig. 11) after 50 missions. After application of the bulk density correlation, the equivalent ratio was 1.19. The most significant point to be made about this correlation is that it suggests that bulk density can be used to predict the relative performance of a TEOS-coated RCC part. Since bulk density can be determined nondestructively, a useful predictive tool for performance of a given RCC segment is possible.

CONCLUDING REMARKS

The two major objectives of this study of mass loss in reinforced carbon-carbon (RCC) material coated with tetraethyl orthosilicate (TEOS) after exposure to simulated Shuttle reentry missions have been achieved. First, stress levels up to 6.8 MPa (980 psi) did not significantly affect the mass-loss

characteristics of TEOS-coated RCC material for temperatures up to 900 K (1160° F). Second, mass-loss data have been obtained for TEOS-coated RCC when temperatures, oxygen partial pressures, and stresses encountered at the lug attachment area of the Shuttle wing leading edge during entry were simultaneously applied to the material. In addition, two important conclusions can be reached as a result of this study:

1. Overall mass loss can be correlated with bulk density of the TEOS-coated RCC material. Since bulk density can be determined nondestructively, a useful predictive tool for performance of a given RCC segment is possible.

2. The previous mass-loss prediction equation was shown to be inadequate in temperature and pressure range encountered in the lug area. The prediction equation was modified as a result of this study. The modified equation adequately predicted the experimentally observed mass loss.

Langley Research Center
National Aeronautics and Space Administration
Hampton, VA 23665
May 8, 1980

APPENDIX A

MEASUREMENT OF TEOS-COATED RCC SPECIMENS

To determine both surface area and bulk volume, the dimensions shown in figure 17 were determined. The linear measurements were made with flat anvil micrometers. Shoulder radius measurements $r_{1,2,3,4}$ were made by comparison with blocks having radii of 72.4 mm (2.85 in.), 73.7 mm (2.90 in.), and 74.9 mm (2.95 in.). The radii were determined to be 73.7 mm (2.90 in.) for all specimens. To preclude coating damage, the diameters of the two pull holes were not measured. All pull holes were assumed to have the nominal dimensions (a diameter of 12.7 mm (0.5 in.)). The dimensions of all specimens are shown in table I.

The specimens were weighed in the as-received condition and after drying overnight. The results of these measurements are presented in table II along with the calculated values for bulk volume, bulk density, surface area, effective cross-sectional area, and weighted thickness.

Bulk volume was computed using a calculated planform area and an average thickness that was weighted with respect to the area between thickness measurements:

$$V_b = A_p t_w \tag{A1}$$

where

A_p calculated planform area, cm^2

V_b bulk volume, cm^3

$$t_w = \frac{A_1(t_1 + t_2)}{2} + \frac{A_2(t_2 + t_3 + t_4)}{3} + \frac{A_3(t_4 + t_5)}{2} \tag{A2}$$

A_1 $= A_3 = 7/16$

A_2 $= 1/8$

t_i thickness, cm

APPENDIX B

MEASUREMENT OF CARBON DIOXIDE CONCENTRATION IN EFFLUENT TEST CHAMBER GAS

The carbon dioxide (CO_2) concentration of the air in the test chamber was sampled continuously from a point immediately adjacent to the surface of the RCC specimens. These samples were taken over a pressure range from 0.1 kPa to 101.1 kPa (0.7 torr to 760 torr). The sampling was accomplished by drawing test chamber air through a CO_2 analyzer with a separate vacuum pump. The test chamber was isolated from the vacuum pump below a pressure of 0.1 kPa (0.7 torr) by a computer-controlled valve. The output of the analyzer was recorded on a strip chart.

The calibration of the sampling system was accomplished in the following manner. A gas mixture of nitrogen and CO_2 with a CO_2 concentration of 0.00656 by volume was pumped through the analyzer. The span was adjusted until the analyzer reading was 65.6 percent of full scale. Since the output of the analyzer was a linear function of CO_2 concentration, full scale corresponded to 1.0 percent CO_2.

The output of the CO_2 analyzer is affected by both pressure levels and mass flow rates. Since the pressure and flow rate vary continuously during a mission profile, the output of the analyzer varies continuously when a fixed concentration of CO_2 is pumped through the system. These factors are complicated by a lag time in the analysis of from 10 to 40 seconds from the time gas is introduced into the test chamber. These uncertainties were resolved by running a calibration mission using a gas mixture of nitrogen and CO_2 (0.656 percent CO_2) as a test medium instead of air. The calibration mission was run at room temperature with RCC specimens removed but duplicated the lug test series pressure profiles.

Figure 18 shows the output of the CO_2 monitor as a function of mission time for the calibration mission cycle. A composite curve was constructed by taking readings at intervals throughout each of the 260 lug missions. The maximum envelope of these recorded CO_2 concentrations is also shown in figure 18. The maximum envelope curve is seen to lie below the calibration mission at every time. Thus, CO_2 concentration in the effluent gas never exceeded 0.656 percent during the lug test series.

Following completion of all lug tests, a calibration check was performed. This check revealed that the recorded output of the analyzer had decreased to 97 percent of the previous value. The calibration check confirmed that large changes did not occur in the measuring system during the test series.

APPENDIX C

SYSTEM PREPARATION DETAILS

Preliminary Tests

Prior to system calibration, some preliminary oxidation testing was conducted to demonstrate that the multiparameter test system provided adequate airflow at all temperatures and pressures to prevent a buildup of oxidation products which could shield TEOS-coated RCC materials from an oxidizing environment. These tests, run with both graphite and RCC coupons, established the following:

1. The vacuum pumping system provides approximately 10 times the airflow required to maintain the free oxygen content in the chamber at a level at least 95 percent of the atmospheric concentration when three TEOS-coated RCC specimens are tested simultaneously. Test results with graphite coupons showed that the CO_2 in the effluent gas never exceeded 2 percent. Initially, carbon monoxide was also monitored. Monitoring of carbon monoxide was discontinued when the levels were found to be consistently low (<2 ppm).

2. The air dryer installed in the system for the TEOS-coated RCC tests was adequate to meet the dew point requirements. The dew point of the chamber inlet air was measured with an electrolytic hygrometer. Constant monitoring over a period of weeks showed that the dew point of the dried air was always less than 218 K (-70° F). These determinations were made at flow rates approximately 4 times maximum vacuum pump capabilities or about 40 times the anticipated maximum flow requirements. Thus, dew points in the chamber were significantly lower than 218 K (-70° F) during the tests.

Temperature Calibration

Preliminary tests with TEOS-coated RCC coupons and a review of the literature showed direct measurement of the temperature of RCC specimens to be extremely difficult. Reproducible temperature measurements were not obtained until platinum/platinum-13% rhodium thermocouples were embedded in the material. Embedding thermocouples in each test specimen was not feasible since the procedure would destroy the integrity of the coating. An alternative approach was to embed thermocouples into a control specimen. TEOS-coated RCC specimen 2 was used exclusively for temperature control. In determining the temperature of the two test locations (A and B) as a function of the temperature at the control location (see fig. 5), two graphite calibration specimens were machined to the same nominal dimensions as the TEOS-coated RCC specimens. The calibration specimens were each instrumented with five platinum/platinum-13% rhodium thermocouples. Holes were drilled into the sides of the calibration specimens so that the bare thermocouple bead contacted the graphite at the centerline of the specimen. (See fig. 6.) A ceramic cement fillet was applied where the thermocouple insulators emerged from the specimen in order to hold the thermocouples in place.

With the graphite calibration specimens in locations A and B and the TEOS-coated RCC control specimen in the third location in the furnace, the control signal of the temperature profile was adjusted until the temperature histories at both A and B were as close as possible to the nominal profile. Because of the effects of air pressure on the heat transfer to the specimens, the nominal mission air pressure profile was maintained during adjustments to the temperature profile.

The results of a typical calibration run after final adjustments of the temperature profile are shown in figure 19. Although the temperature profiles on both calibration specimens are close to the nominal, the changing temperature distribution along the length of the specimens as a function of mission time precluded further adjustments of the command signal to get a more uniform temperature distribution.

Pressure Calibration

For calibration of the pressure profile, the local pressure at the specimen location was assumed to be the same as that at the system pressure sensor. This assumption is reasonable since the pressure changes in the profile are not rapid and the pressure chamber has no significant baffles. The pressure sensor is a capacitance-type transducer whose inlet port is located on a cold wall of the vacuum chamber approximately 200 mm (8 in.) from the center of the heated zone.

The results of the system air pressure calibration are shown in figure 20. During most of the mission profile, the chamber air pressure was within the desired tolerance. The short periods when the pressure was out of tolerance were a result of the closing and/or opening of the pressure control solenoid valves. These valves are necessary to limit the flow of the pressurized (approximately 21 kPa (3 psi)) inlet air to the servo-controlled needle valves which control chamber air pressure. Chamber pressure returns to nominal as soon as the servo valves can respond to the pressure surge caused by the solenoid valves. Air pressure errors were minimized by interactively adjusting the pressure command signal, the timing of the solenoid valve operation, and the amount of vacuum pumping on the vacuum chamber.

Load Calibration

The load trains for locations A and B were calibrated using a load cell which had been calibrated using National Bureau of Standards traceable deadweights. Load profile calibration curves demonstrated that the load control consistently held the load on the specimens within the desired tolerance.

Calibration Missions

To assess the effect of temperature and pressure control on the adequacy of mission simulation, a series of five simulated mission cycles was applied to

the graphite calibration specimens. During these mission profiles, chamber pressure and specimen temperature were recorded every 24 seconds. Using these data and the nominal mission profile, the expected mass loss of the TEOS-coated RCC specimens was calculated. These calculations used the Vought 1976 mass-loss prediction equation presented in appendix D (eq. (D1)). This equation treats mass loss of TEOS-coated RCC as a single-valued exponential function of temperature. This treatment amplifies the effect of slight temperature differences during a mission and provides an excellent check of reproducibility. Note that absolute correctness of the prediction equation is not required to check reproducibility. The calculated mass loss for each thermocouple location is presented in figure 21 for one mission cycle. Also plotted is the mass loss when a nominal trajectory is used and the bounds on calculated mass loss when the trajectory deviates above and below the nominal by the tolerances set on temperature and pressure. For both chamber locations, the calculated mass loss for all points falls within the bounds set by the temperature and pressure tolerance limits. The calculated mass loss is considered a reasonable measure of the degree of simulation achieved during a particular mission cycle. This assumption was used to measure the degree of reproducibility in the set of five mission profile calibration runs. These calibration cycles were exact duplicates of the subsequent TEOS-coated RCC test series. Five mission cycles were run in a single day under complete computer control. A summary of the results of these calibration cycles is shown in table V.

Table V lists mass loss calculated at the 10 thermocouple locations in the graphite calibration specimens. One mass loss was computed for each of five mission simulation cycles. Also shown is the mass loss computed using a nominal mission profile and using the upper and lower tolerance boundaries for temperature and air pressure. The mass losses computed at various points along the specimen show sizable variation, but all points are well within the maximum and minimum tolerance boundaries. Mission-to-mission comparisons at a single point show that reproducibility was excellent. As would be expected, the averages from mission-to-mission show small variation. The averages for five thermocouple locations, averaged over five mission cycles produce one average number for location A and one average number for location B. When these averages are compared with the nominal, location A has a computed mass loss 5 percent higher than nominal; location B, 5 percent lower than the nominal.

These five calibration missions were repeated during the middle of the test series and again at the end of testing. A comparison of these missions with the initial calibration missions verified that the quality of simulation remained high throughout the test series.

Test Procedure

Two TEOS-coated RCC specimens were tested simultaneously for each test series. The location (A or B) of the loaded specimen was alternated with each test series. The control specimen remained in place in the third position as previously described. The test series used the same procedures as the calibration missions previously described. The specimens were subjected to five mission cycles each day. These missions were under complete computer control with

no operator intervention. The procedure described below took approximately 11 hours each day.

The following procedure was used each day that testing was in progress. All specimens were handled with plastic gloves to prevent contamination.

1. Instrumentation was checked.

2. Both test specimens were removed, placed in the desiccator, and transported to an analytical balance.

3. Specimen A was weighed first (to the nearest milligram), followed by specimen B.

4. Specimens A and B were transported in the desiccator to the photographic station.

5. Specimen A was removed from the desiccator and photographed on both sides. Specimen B was then photographed. Both were transported back to the vacuum chamber in a desiccator.

6. Specimen A was reinstalled in the load train. Specimen B was then reinstalled. (Installation order was reversed on the succeeding day.)

7. The chamber was sealed, and the load servo controls were activated.

8. The data recording procedure was initialized.

9. The master-control computer program was started.

The master-control computer program took complete control for the remainder of the time. At the completion of five simulated missions, the operator intervened and used manual switches to reduce the chamber pressure to 8 Pa (60 mtorr). An additional computer program was called up by the operator to set the temperature of the control specimen to 343 K (158^{o} F). These constant environmental conditions were maintained until the start of the next mission cycle. No effect of length of time between mission cycles was noted in the mass-loss data.

APPENDIX D

VOUGHT CORPORATION MASS-LOSS PREDICTION EQUATION

Equation (D1) is the mass-loss prediction equation used during the experiments reported herein. This equation was derived by the Vought Corporation (unpublished data) and was verified by Johnson Space Center as the one being used for shuttle design during the test series described herein.

$$\dot{m} = \dot{m}_D P^n \left\{ \frac{1 + m_L K_4 \exp\left(E_4/RT\right)}{\left[1 + K_1 \exp\left(E_1/RT\right)\right]\left[1 + K_3 \exp\left(E_3/RT\right)\right]} - \frac{1}{1 + K_2 \exp\left(E_2/RT\right)} \right\} \quad \text{(D1)}$$

where

$\dot{m}$ mass loss rate, kg/m^2-s (lb/ft^2-sec)

m_L accumulated mass loss, kg/m^2 (lb/ft^2), $\int_0^t \dot{m}\, dt$, where t is mission time in seconds

$\dot{m}_D = 1.464 \times 10^{-5} \frac{kg}{m^2\text{-s-atm}^n} \left(3.055 \times 10^{-6} \frac{lb}{ft^2\text{-sec-atm}^n} \right)$

$K_1 = 4.1645 \times 10^{-5}$

$\frac{E_1}{R} = 8993.33$ K (16 188° R)

$K_2 = 4.119 \times 10^{-6}$

$\frac{E_2}{R} = 17\ 362.78$ K (31 253° R)

$K_3 = 2.4755 \times 10^{-26}$

$\frac{E_3}{R} = 40\ 500$ K (72 900° R)

$K_4 = 1.2727 \times 10^{-2}$

$\frac{E_4}{R} = 5595.35$ K (10 071.63° R)

P pressure, atm

T temperature, K (°R)

$n = 0.8$ for $T \geq 1255$ K (2260° R)

n $= 0.7907 - 2.018P$ for $T < 1255$ K (2260° R) and $P < 0.3918$ atm

n $= 0$ for $T < 1255$ K (2260° R) and $P \geq 0.3918$ atm

Once the experimental results reported herein were communicated to Vought Corporation, equation (D1) was modified by Vought Corporation (unpublished data), as follows:

$$\dot{m} = \dot{m}'_D P^{n'} \left\{ \frac{1 + Bm_L}{\left[1 + K'_1 \exp\left(E'_1/RT\right)\right]\left[1 + K'_3 \exp\left(E'_3/RT\right)\right]} - \frac{1}{1 + K'_2 \exp\left(E'_2/RT\right)} \right\} \quad \text{(D2)}$$

where

$\dot{m}$ mass-loss rate, kg/m^2-s (lb/ft^2-sec)

m_L accumulated mass loss, kg/m^2 (lb/ft^2), $\int_0^t \dot{m}\, dt$, where t is mission time in seconds

$\dot{m}'_D$ $= 1.367 \times 10^{-5} \frac{kg}{m^2\text{-s-atm}^n} \left(28.0 \times 10^{-7} \frac{lb}{ft^2\text{-sec-atm}^n}\right)$

B $= -7.324 + \frac{20\ 300\ K}{T} = \left(-7.324 + \frac{36\ 540^{\circ}\ R}{T}\right)$

K'_1 $= 9.231 \times 10^{-6}$

$\frac{E'_1}{R}$ $= 9811$ K ($17\ 660^{\circ}$ R)

K'_2 $= 6.135 \times 10^{-6}$

$\frac{E'_2}{R}$ $= 15\ 183.33$ K ($27\ 330^{\circ}$ R)

K'_3 $= 2.84 \times 10^{-9}$

$\frac{E'_3}{R}$ $= 12\ 177.78$ K ($21\ 920^{\circ}$ R)

n' $= 0.62$

P pressure, atm

T temperature, K ($^{\circ}$R)

REFERENCES

1. Medford, J. E.: Multi-Cycle Plasma Arc Evaluation of Oxidation Inhibited Carbon-Carbon Material for Shuttle Leading Edges. ASME Paper 72-ENAv-26, Aug. 1972.

2. McGinnis, F. K.: Shuttle LESS Subsurface Attack Investigation. NASA CR-155520, 1974.

3. Medford, J. E.: Prediction of Oxidation Performance of Reinforced Carbon-Carbon Material for Space Shuttle Leading Edges. AIAA Paper No. 75-730, May 1975.

4. Dicus, Dennis L.; Hopko, Russell N.; and Brown, Ronald D.: Ablative Performance of Uncoated Silicone-Modified and Shuttle Baseline Reinforced Carbon Composites. NASA TN D-8358, 1976.

5. Curry, Donald M.; Johansen, K. J.; and Stephens, Emily W.: Reinforced Carbon-Carbon Oxidation Behavior in Convective and Radiative Environments. NASA TP-1284, 1978.

6. Standard for Metric Practice. E 380-76, American Soc. Testing & Mater., 1976.

7. Miller, Irwin; and Freund, John E.: Probability and Statistics for Engineers. Prentice-Hall, Inc., c.1965.

TABLE I.- DIMENSIONS OF TEOS-COATED RCC SPECIMENS

(a) SI Units

Specimen	Thickness					Length
	t_1', mm	t_2', mm	t_3', mm	t_4', mm	t_5', mm	ℓ, mm
1	9.921	10.003	9.987	9.987	10.005	221.88
3	10.013	10.102	10.058	10.069	10.033	221.88
4	9.936	10.033	10.053	10.038	10.066	223.20
5	9.944	10.041	10.036	10.056	10.043	221.82
6	9.919	10.028	9.952	10.013	10.030	221.98
7	9.934	9.987	10.028	10.033	10.023	221.95
8	9.832	9.888	9.936	9.936	9.952	221.89
9	9.962	9.977	9.975	9.987	10.008	221.81

Specimen	Width						
	w_1', mm	w_2', mm	w_3', mm	w_4', mm	w_5', mm	w_6', mm	w_7', mm
1	43.318	43.409	17.876	17.871	17.882	43.409	43.396
3	43.437	43.490	17.810	17.818	17.831	43.485	43.523
4	43.462	43.485	17.882	17.871	17.869	43.482	43.485
5	43.411	43.459	17.861	17.877	17.866	43.439	43.457
6	43.434	43.464	17.871	17.861	17.851	43.470	43.459
7	43.464	43.485	17.795	17.805	17.800	43.490	43.480
8	43.444	43.472	17.805	17.775	17.729	43.477	43.477
9	43.462	43.454	17.887	17.882	17.904	43.467	43.459

TABLE I.- Concluded

(b) U.S. Customary Units

Specimen	Thickness					Length
	t_1, in.	t_2, in.	t_3, in.	t_4, in.	t_5, in.	ℓ, in.
1	0.3906	0.3938	0.3932	0.3932	0.3939	8.7353
3	.3942	.3977	.3960	.3964	.3950	8.7353
4	.3912	.3950	.3958	.3952	.3963	8.7358
5	.3915	.3953	.3951	.3959	.3954	8.7331
6	.3905	.3948	.3918	.3942	.3949	8.7357
7	.3911	.3932	.3948	.3950	.3946	8.7382
8	.3871	.3893	.3912	.3912	.3918	8.7327
9	.3922	.3928	.3927	.3932	.3940	8.7357

Specimen	Width						
	w_1, in.	w_2, in.	w_3, in.	w_4, in.	w_5, in.	w_6, in.	w_7, in.
1	1.7078	1.7090	0.7038	0.7036	0.7040	1.7090	1.7085
3	1.7101	1.7122	.7012	.7015	.7020	1.7120	1.7135
4	1.7111	1.7120	.7040	.7036	.7035	1.7119	1.7120
5	1.7091	1.7110	.7032	.7038	.7034	1.7102	1.7109
6	1.7100	1.7112	.7036	.7032	.7028	1.7114	1.7110
7	1.7112	1.7120	.7006	.7010	.7008	1.7122	1.7118
8	1.7104	1.7115	.7010	.6998	.6980	1.7117	1.7117
9	1.7111	1.7108	.7042	.7040	.7049	1.7113	1.7109

TABLE II.- PHYSICAL CHARACTERISTICS OF TEOS-COATED RCC SPECIMENS

(a) SI Units

Specimen	As-received weight, g	Weight after drying, g	Bulk volume, cm^3	Bulk density, g/cm^3	Calculated surface area, m^2	Effective cross-sectional area, mm^2	Weighted thickness, t_w, mm
1	107.910	107.321	66.301	1.6187	0.01867	158.3	9.980
3	107.579	107.043	66.802	1.6024	.01873	159.1	10.056
4	107.713	107.206	66.641	1.6087	.01873	159.1	10.020
5	107.965	107.385	66.587	1.6127	.01871	159.6	10.020
6	107.685	107.152	66.447	1.6126	.01876	158.3	9.997
7	107.273	106.758	66.392	1.6080	.01870	157.9	9.997
8	107.352	106.748	65.715	1.6244	.01863	156.1	9.903
9	108.214	107.593	66.362	1.6213	.01869	158.3	9.982

TABLE II.- Concluded

(b) U.S. Customary Units

Specimen	As-received weight, lb	Weight after drying, lb	Bulk volume, ft^3	Bulk density, lb/ft^3	Calculated surface area, ft^2	Effective cross-sectional area, in^2	Weighted thickness, t_w, in.
1	0.237901	0.236602	2.3411×10^{-3}	101.06	0.2012	0.2454	0.3929
3	.237171	.235989	2.3601	99.99	.2016	.2466	.3959
4	.237467	.236349	2.3545	100.38	.2016	.2466	.3945
5	.238022	.236743	2.3526	100.63	.2014	.2465	.3945
6	.237405	.236230	2.3477	100.62	.2013	.2453	.3936
7	.236496	.235361	2.3456	100.34	.2013	.2448	.3936
8	.236671	.235339	2.3218	101.36	.2006	.2420	.3899
9	.238571	.237202	2.3466	101.17	.2012	.2453	.3930

TABLE III.- NOMINAL MISSION PROFILE OF LUG ATTACHMENT AREA

Time, s	Temperature	
	K	^{o}F
0	394	250
300	404	268
400	415	287
500	446	343
600	491	425
800	594	609
1000	685	774
1200	764	915
1400	826	1027
1500	848	1067
1600	863	1094
1700	871	1109
1800	874	1114
1900	871	1108
2000	863	1093
2100	850	1070
2200	833	1040
2300	814	1005
2400	794	970
2600	756	901
2800	722	840
3000	691	784
3200	664	735
3400	639	690
3700	605	629
4000	580	585

Time, s	Pressure, atm
0	
1200	$< 10^{-6}$
1400	7×10^{-4}
1600	2.27×10^{-3}
1640	4.84×10^{-3}
1720	9.97×10^{-3}
1760	1.25×10^{-2}
1800	1.50×10^{-2}
1850	3.40×10^{-2}
1900	5.10×10^{-2}
1940	7.70×10^{-2}
1980	0.109×10^{0}
2000	.135
2040	.166
2060	.189
2080	.226
2120	.342
2140	.424
2160	.521
2200	.731
2220	.841
2240	.938
2260	1.000
4000	1.000

Time, s	Stress	
	MPa	psi
0	0	0
1200	6.7569	980
1800	6.7569	980
2200	0	0
4000	0	0

TABLE IV.- SUMMARY OF CUMULATIVE MASS-LOSS DATA

Number of missions	Test series I			
	Specimen 3; location A; load		Specimen 5; location B; no load	
	Mass loss		Mass loss	
	g/m^2	lb/ft^2	g/m^2	lb/ft^2
5	27.78	0.00569	23.68	0.00485
10	54.14	.01109	47.07	.00964
15	85.74	.01756	71.33	.01461
20	119.08	.02439	101.17	.02072
25	154.48	.03164	128.70	.02636
30	190.17	.03895	161.42	.03306
35	230.16	.04714	191.78	.03928
40	271.12	.05553	225.96	.04628
45	313.94	.06430	261.90	.05364
50	356.81	.07308	298.52	.06114

TABLE IV.- Continued

Number of missions	Test series II			
	Specimen 1; location A; no load		Specimen 9; location B; load	
	Mass loss		Mass loss	
	g/m^2	lb/ft^2	g/m^2	lb/ft^2
5	22.26	0.00456	22.02	0.00451
10	52.29	.01071	40.87	.00837
15	69.19	.01417	63.33	.01297
20	94.04	.01926	87.30	.01788
25	121.57	.02490	110.73	.02268
30	149.89	.03070	138.66	.02840
35	179.87	.03684	165.08	.03381
40	210.58	.04313	193.98	.03973
45	243.98	.04997	223.72	.04582
50	276.69	.05667	254.08	.05204
55	310.33	.06356	285.04	.05838
60	345.09	.07068	316.87	.06490
65	379.42	.07771	349.83	.07163
70	417.45	.08550	384.84	.07882
75	444.50	.09104	[a]410.87	.08415
80	491.08	.10058	453.78	.09294

[a]Specimen 9 weighed after 74 missions.

TABLE IV.- Continued

Number of missions	Test series III			
	Specimen 6; location A; load		Specimen 7; location B; no load	
	Mass loss		Mass loss	
	g/m^2	lb/ft^2	g/m^2	lb/ft^2
5	24.90	0.00510	20.60	0.00422
10	43.11	.00883	36.91	.00756
15	66.65	.01365	56.83	.01164
20	91.01	.01864	78.27	.01603
25	116.98	.02396	99.21	.02032
30	144.91	.02968	123.19	.02523
35	174.55	.03575	148.33	.03038
40	204.38	.04186	173.62	.03556
45	233.72	.04787	200.52	.04107
50	266.73	.05463	228.16	.04673

TABLE IV.- Concluded

Number of missions	Test series IV			
	Specimen 4; location A; no load		Specimen 8; location B; load	
	Mass loss		Mass loss	
	g/m^2	lb/ft^2	g/m^2	lb/ft^2
5	26.56	0.00544	21.63	0.00443
10	52.29	.01071	39.11	.00801
15	78.66	.01611	58.69	.01202
20	108.24	.02217	79.05	.01619
25	139.88	.02865	100.73	.02063
30	171.18	.03506	123.58	.02531
35	204.14	.04181	145.74	.02985
40	237.97	.04874	170.84	.03499
45	271.95	.05570	194.47	.03983
50	308.92	.06327	219.37	.04493
55	347.88	.07125	248.42	.05088
60	385.81	.07902	275.13	.05635
65	424.78	.08700	303.89	.06224
70	465.55	.09535	332.55	.06811
75	506.50	.10375	361.30	.07400

TABLE V.- COMPARISON OF CALIBRATION MISSIONS WITH NOMINAL MISSION

(a) Calculated total mass losses during five calibration missions

Mission profile calibration cycle	Mass loss at thermocouple -											
	1		2		3		4		5		Average	
	g/m^2	lb/ft^2	g/m^2	lb/ft^2	g/m^2	lb/ft^2	g/m^2	lb/ft^2	g/m^2	lb/ft^2	g/m^2	lb/ft^2
Furnace location A												
1	3.388	0.694×10^{-3}	3.359	0.688×10^{-3}	3.008	0.616×10^{-3}	2.964	0.607×10^{-3}	3.232	0.662×10^{-3}	3.188	0.653×10^{-3}
2	3.379	.692	3.359	.688	3.008	.616	2.953	.605	3.217	.659	3.183	.652
3	3.374	.691	3.349	.686	3.003	.615	2.959	.606	3.242	.664	3.183	.652
4	3.379	.692	3.354	.687	3.008	.616	2.973	.609	3.252	.666	3.193	.654
5	3.383	.693	3.354	.687	3.008	.616	2.973	.609	3.261	.668	3.198	.655
Average	3.379	.692	3.354	.687	3.008	.616	2.964	.607	3.242	.664	3.188	.653
Furnace location B												
1	2.998	0.614×10^{-3}	2.739	0.561×10^{-3}	2.695	0.552×10^{-3}	3.042	0.623×10^{-3}	3.017	0.618×10^{-3}	2.900	0.594×10^{-3}
2	2.978	.610	2.719	.557	2.680	.549	3.027	.620	3.003	.615	2.881	.590
3	2.978	.610	2.734	.560	2.676	.548	3.022	.619	3.027	.620	2.890	.592
4	2.978	.610	2.734	.560	2.676	.548	3.022	.619	3.027	.620	2.885	.591
5	2.983	.611	2.739	.561	2.680	.549	3.027	.620	3.037	.622	2.895	.593
Average	2.983	.611	2.734	.560	2.680	.549	3.027	.620	3.022	.619	2.890	.592

(b) Calculated total mass losses and tolerance boundaries for nominal mission

Condition	Calculated mass loss	
	g/m^2	lb/ft^2
Nominal mission	3.047	0.624×10^{-3}
Lower tolerance boundary for temperature and pressure	2.436	0.499×10^{-3}
Upper tolerance boundary for temperature and pressure	3.759	0.770×10^{-3}

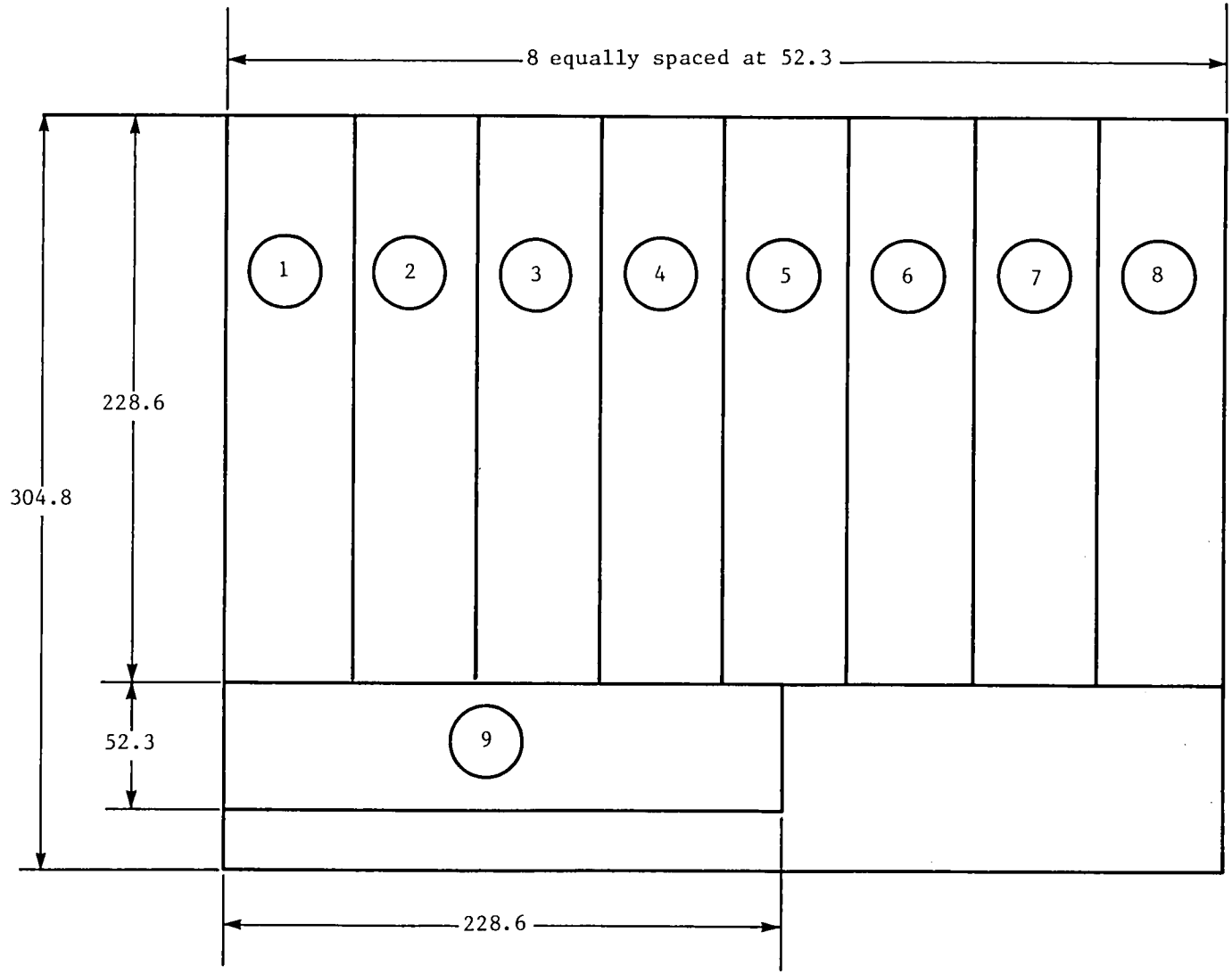

Figure 1.- Specimen layout for 33-ply reinforced carbon-carbon material blanks.
(Dimensions are in millimeters.)

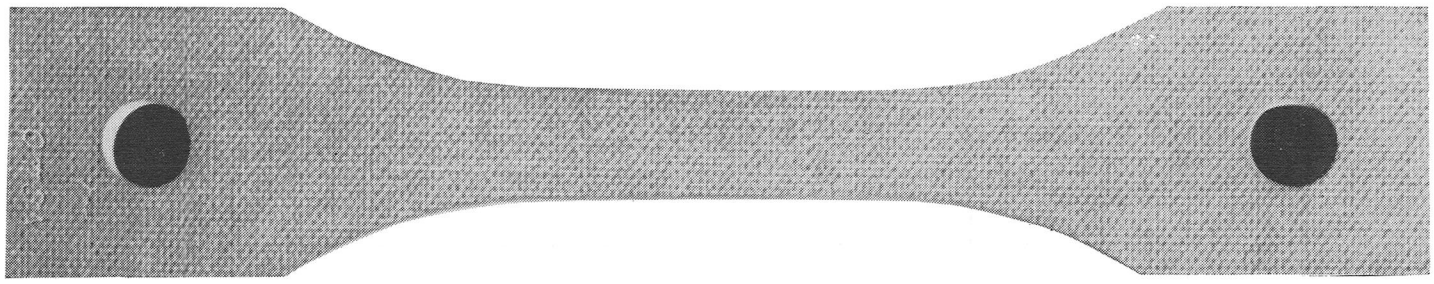

L-77-6212.1

Front

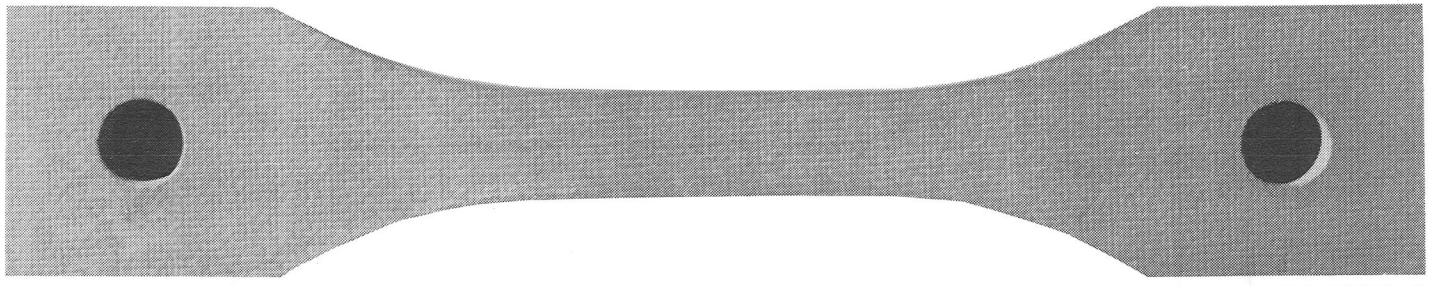

L-77-6215.1

Back

Figure 2.- As-received TEOS-coated RCC specimen 1.

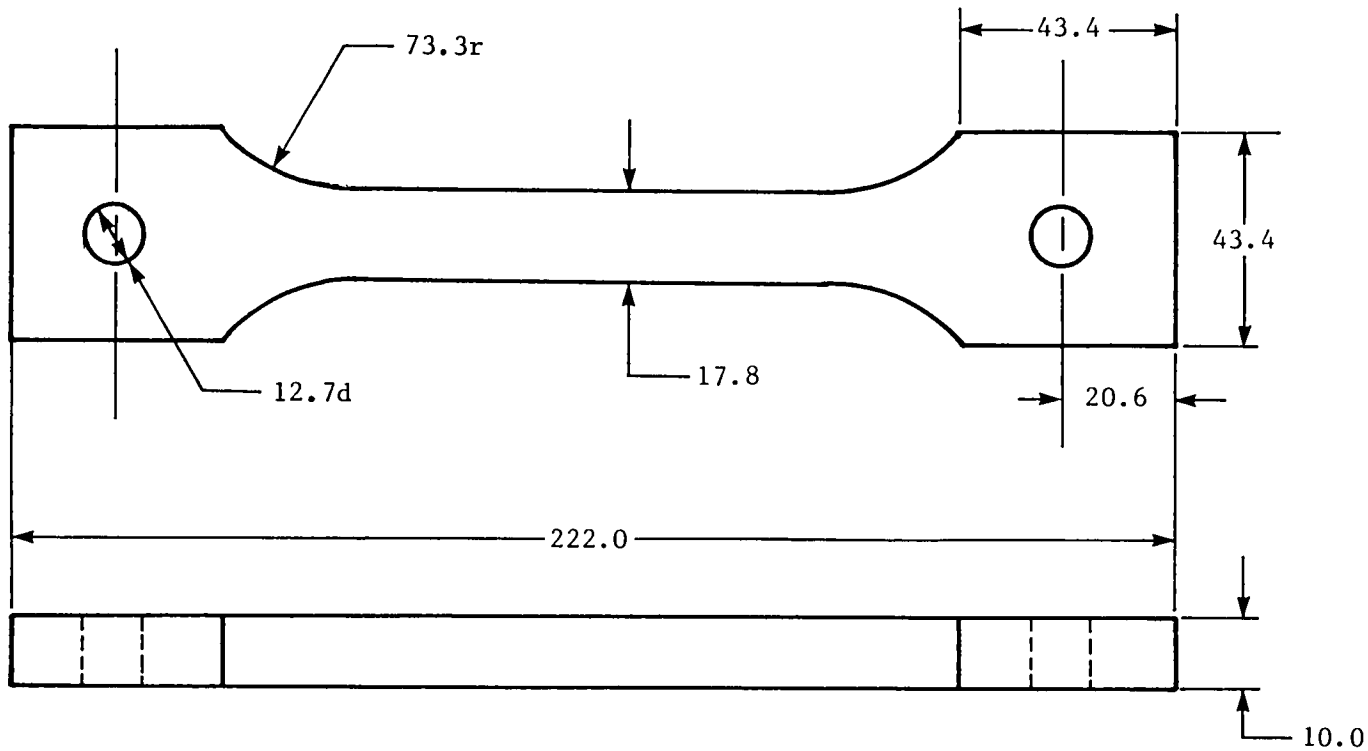

Figure 3.- Nominal dimensions of 33-ply TEOS-coated RCC specimens.
(Dimensions are in millimeters.)

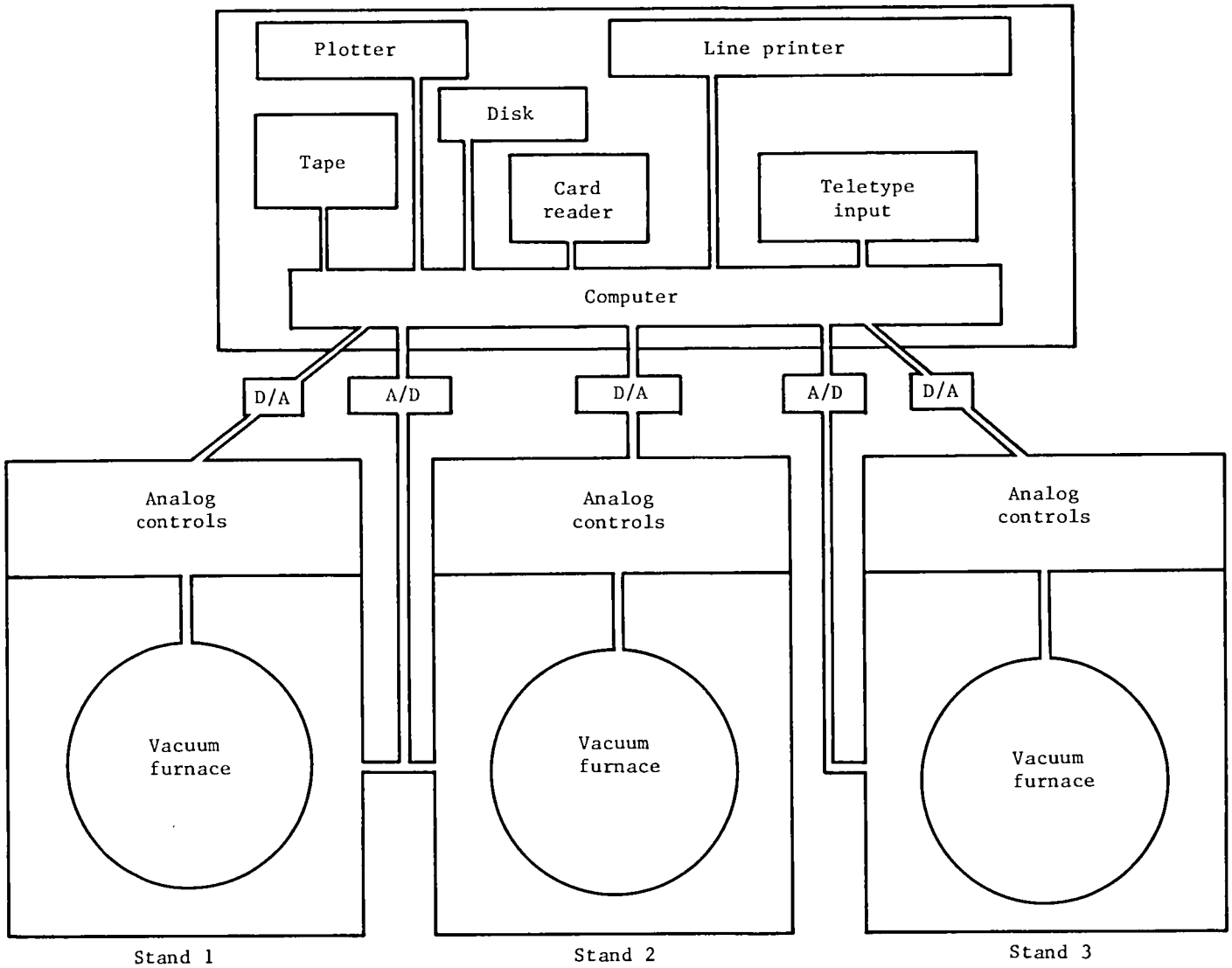

(a) Block diagram.

Figure 4.- Multiparameter test system.

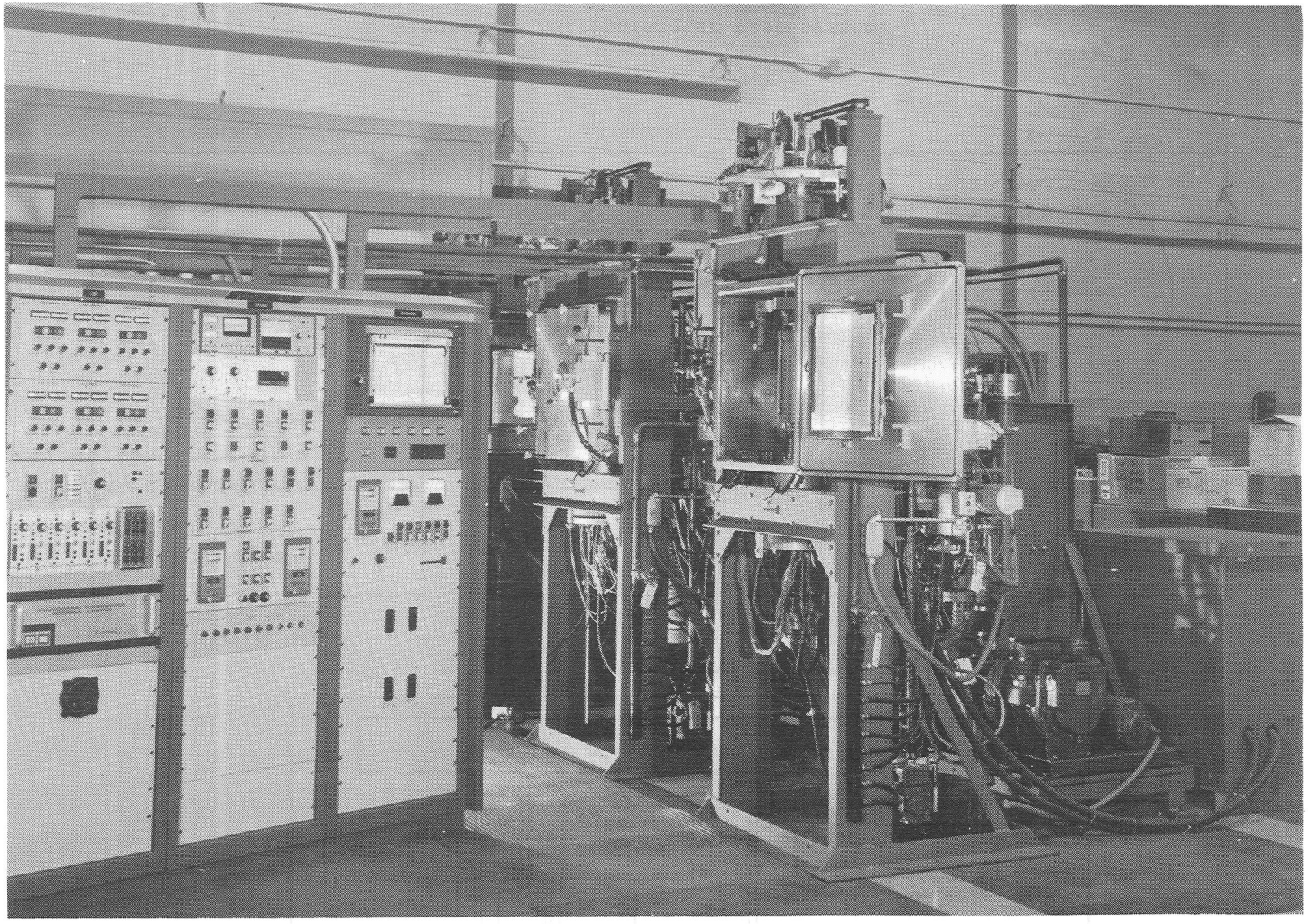

L-80-130

(b) Vacuum furnaces and analog controls.

Figure 4.- Concluded.

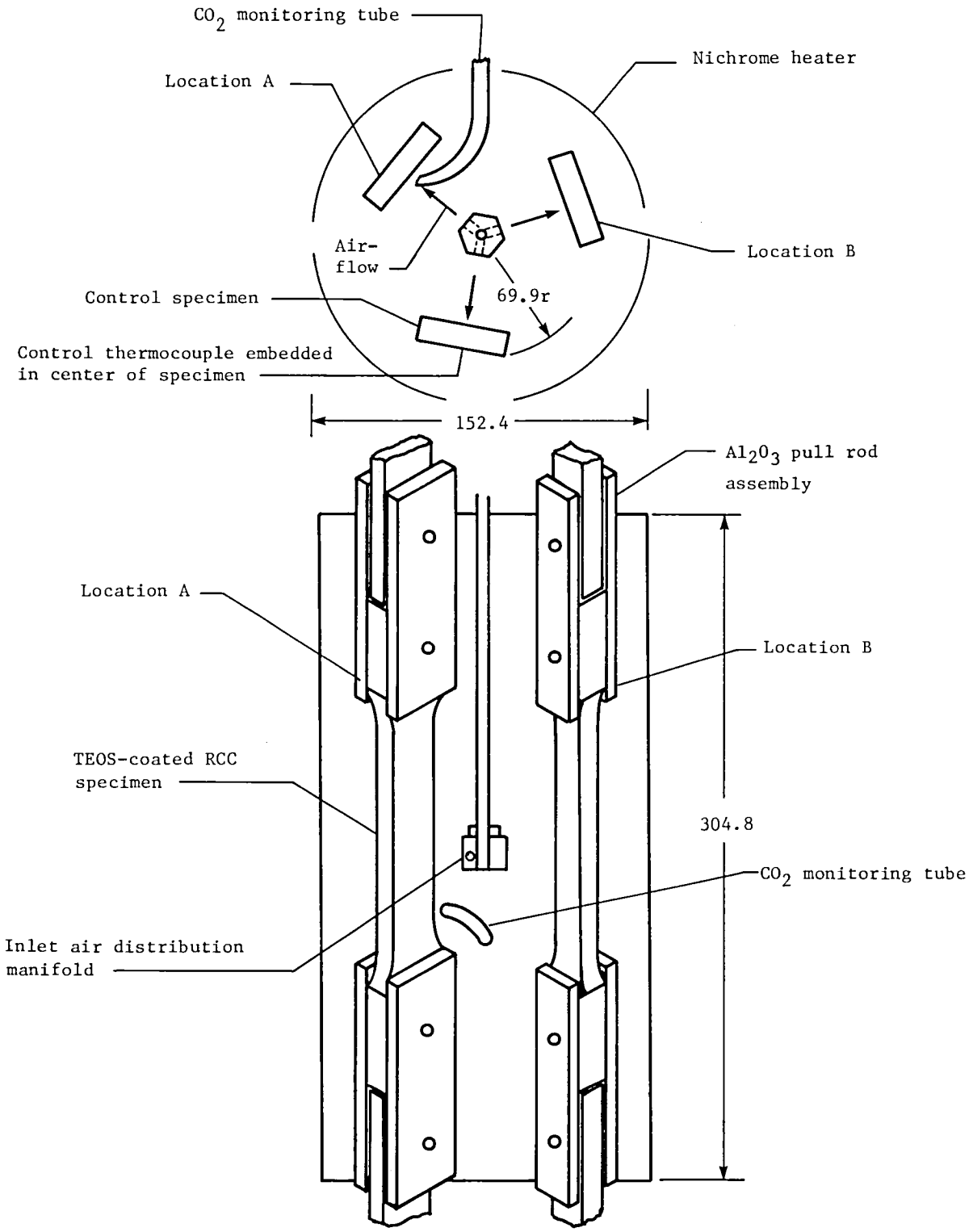

Figure 5.- Furnace and specimen configuration. (Dimensions are in millimeters.)

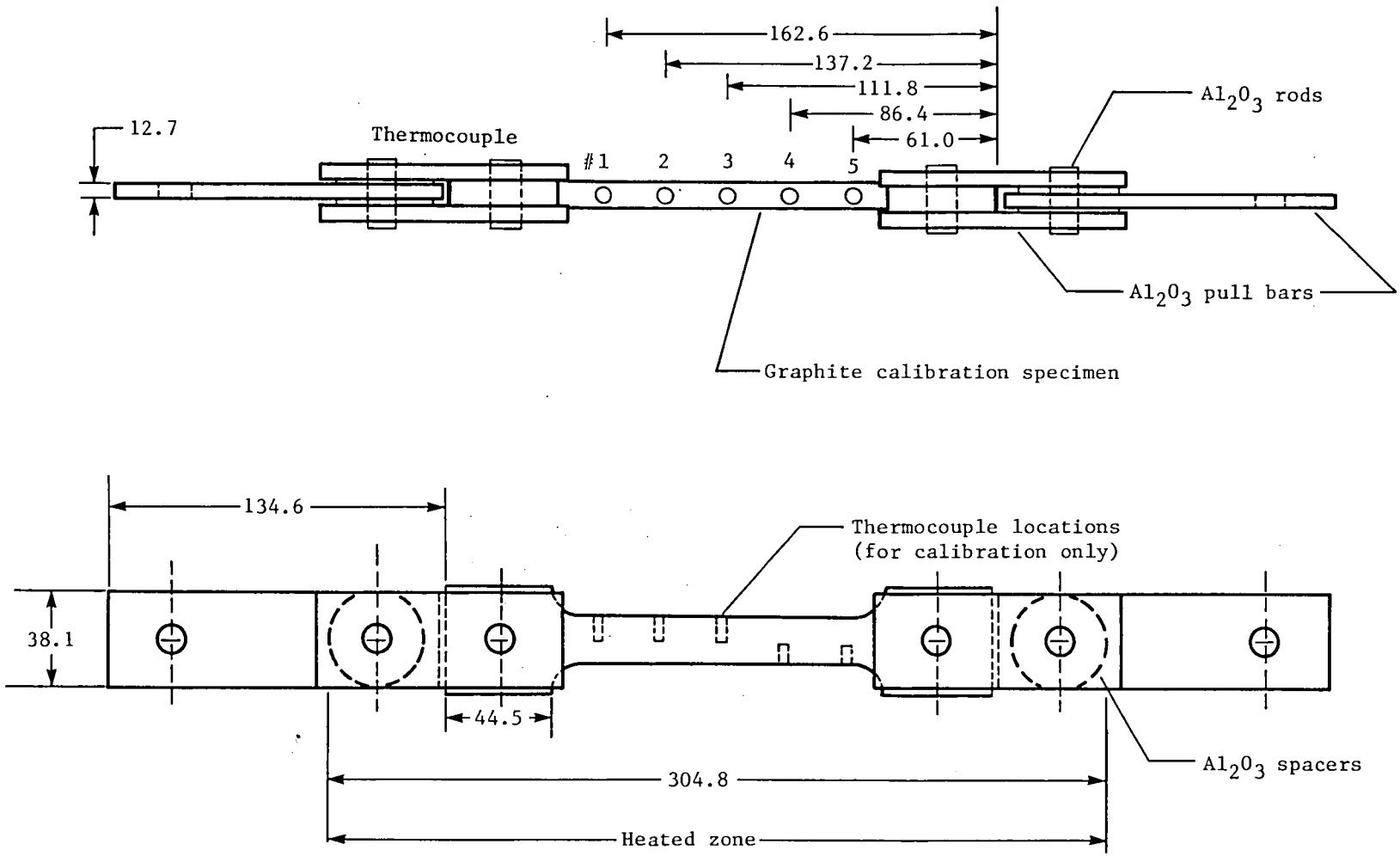

Figure 6.- Load train configuration with calibration specimen in place.
(Dimensions are in millimeters.)

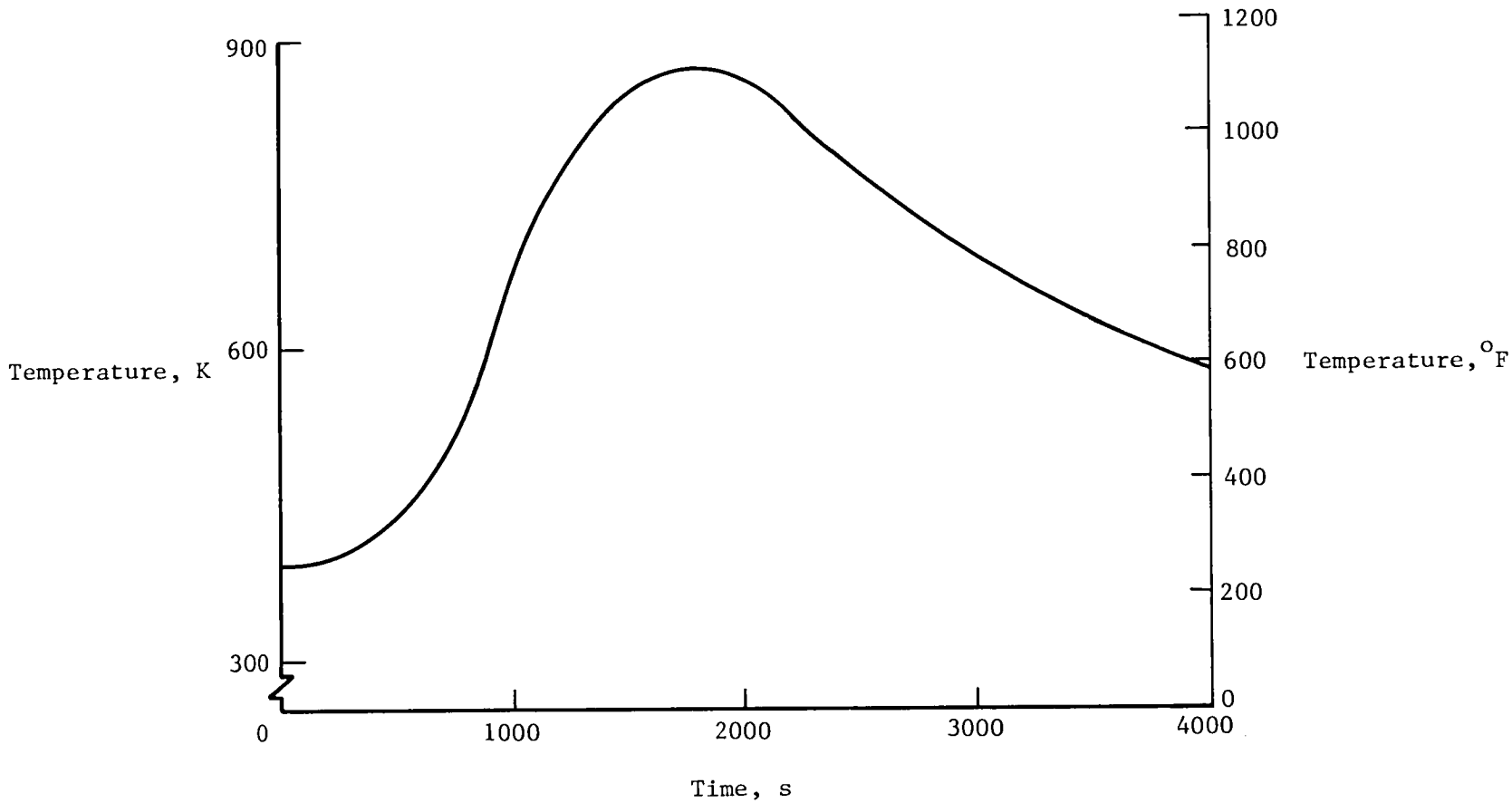

(a) Temperature history.

Figure 7.- Lug area mission histories.

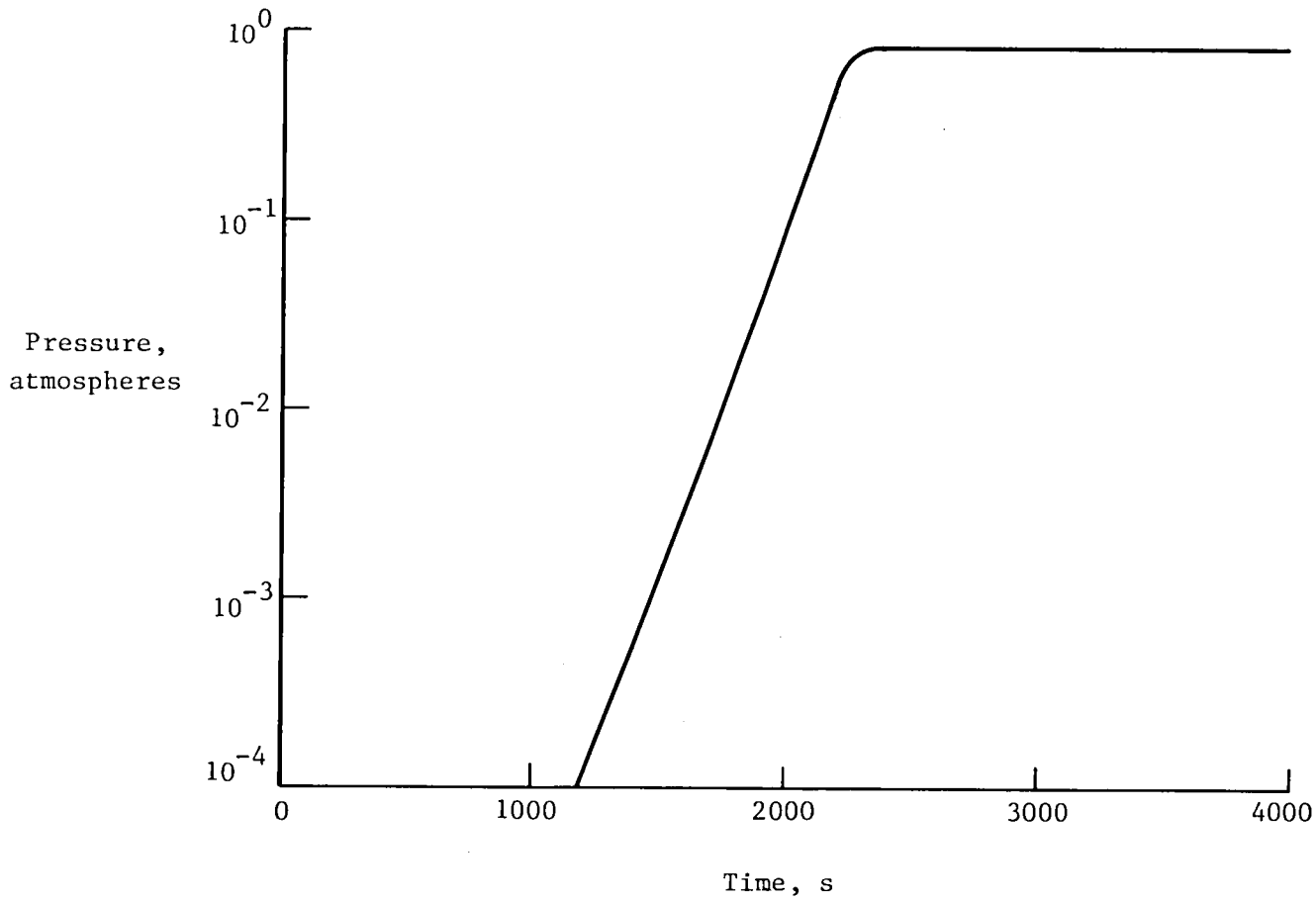

(b) Pressure profile.

Figure 7.- Continued.

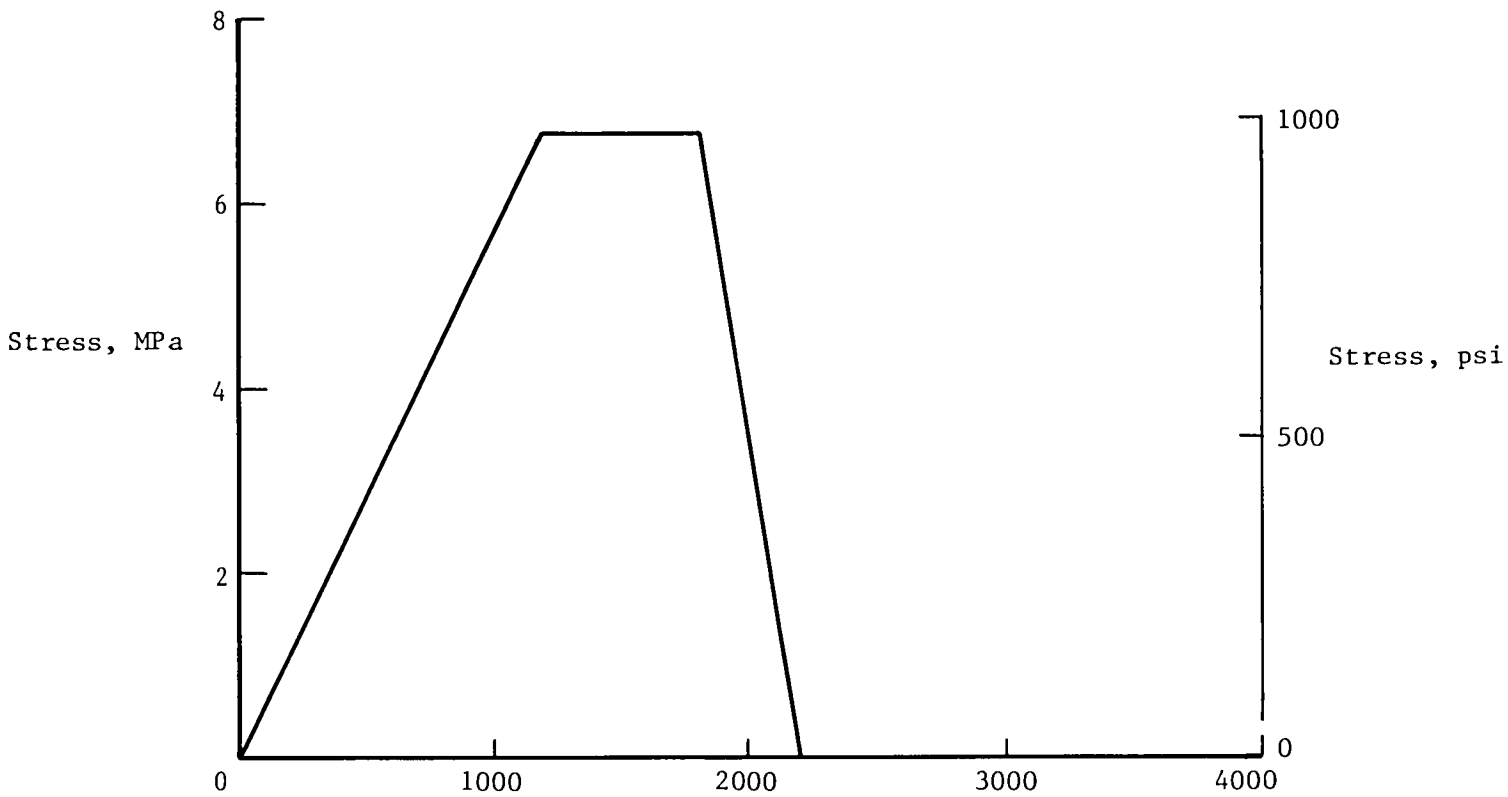

(c) Load profile.

Figure 7.- Concluded.

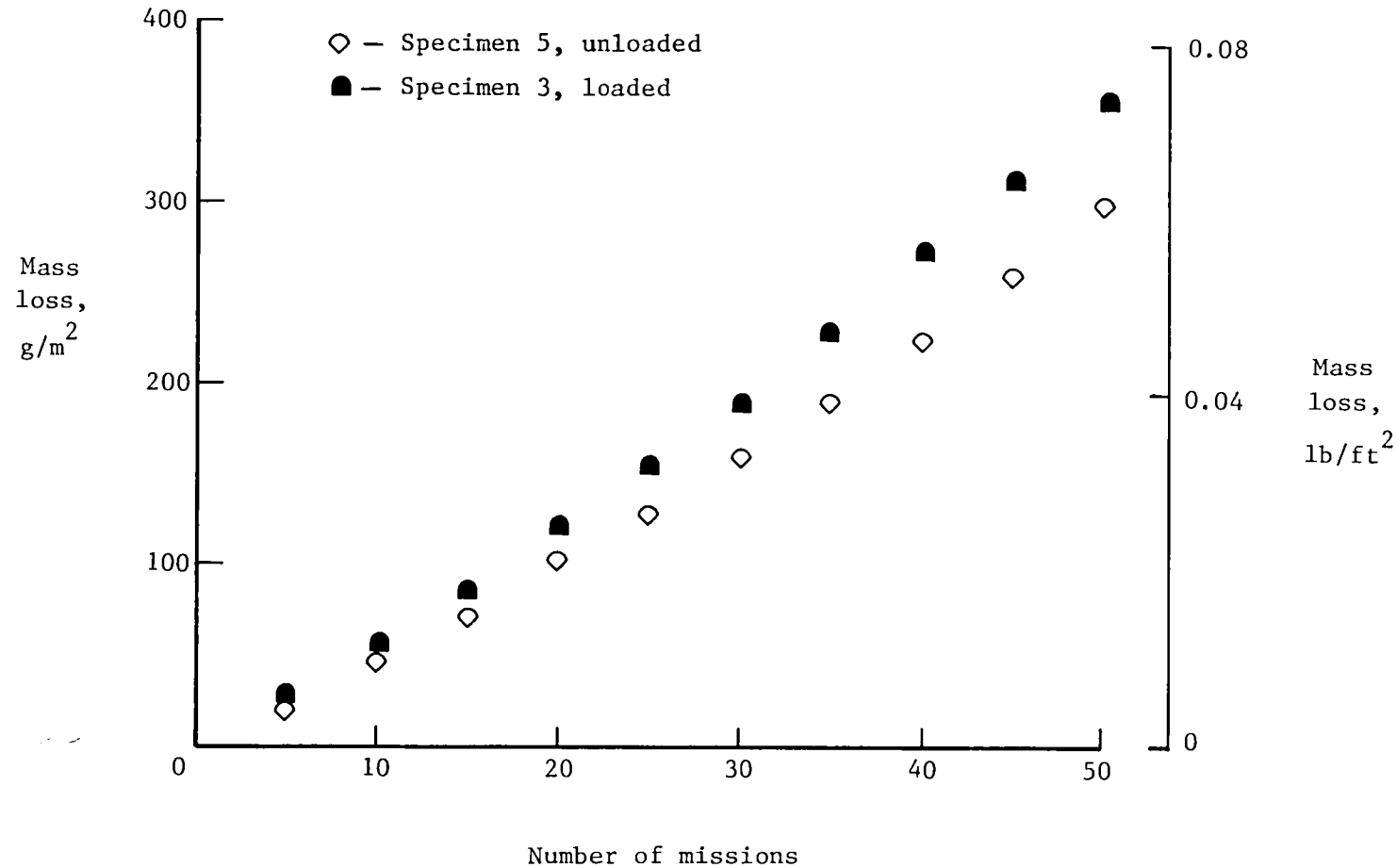

(a) Test series I.

Figure 8.- Mass loss as a function of mission cycles.

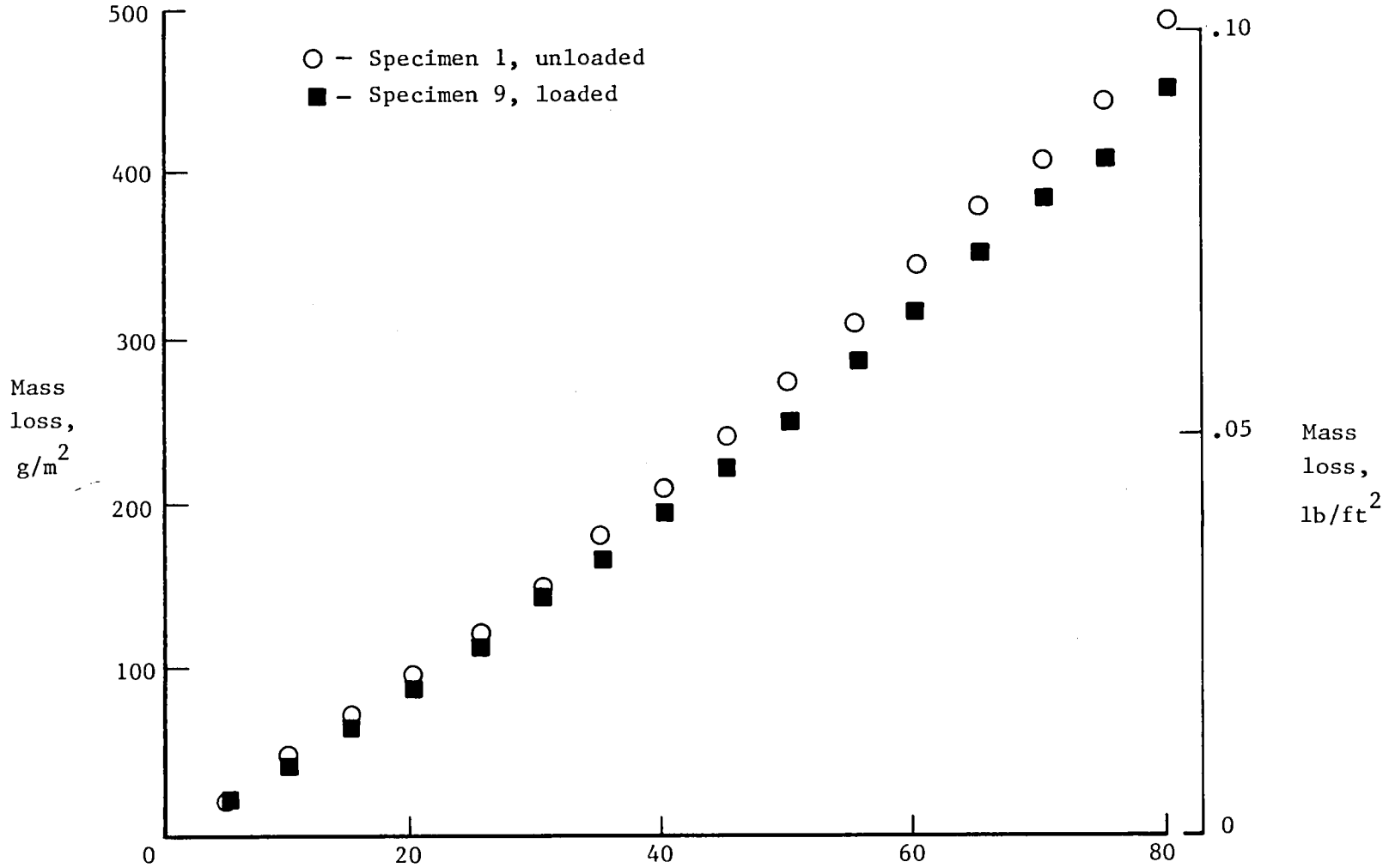

(b) Test series II.

Figure 8.- Continued.

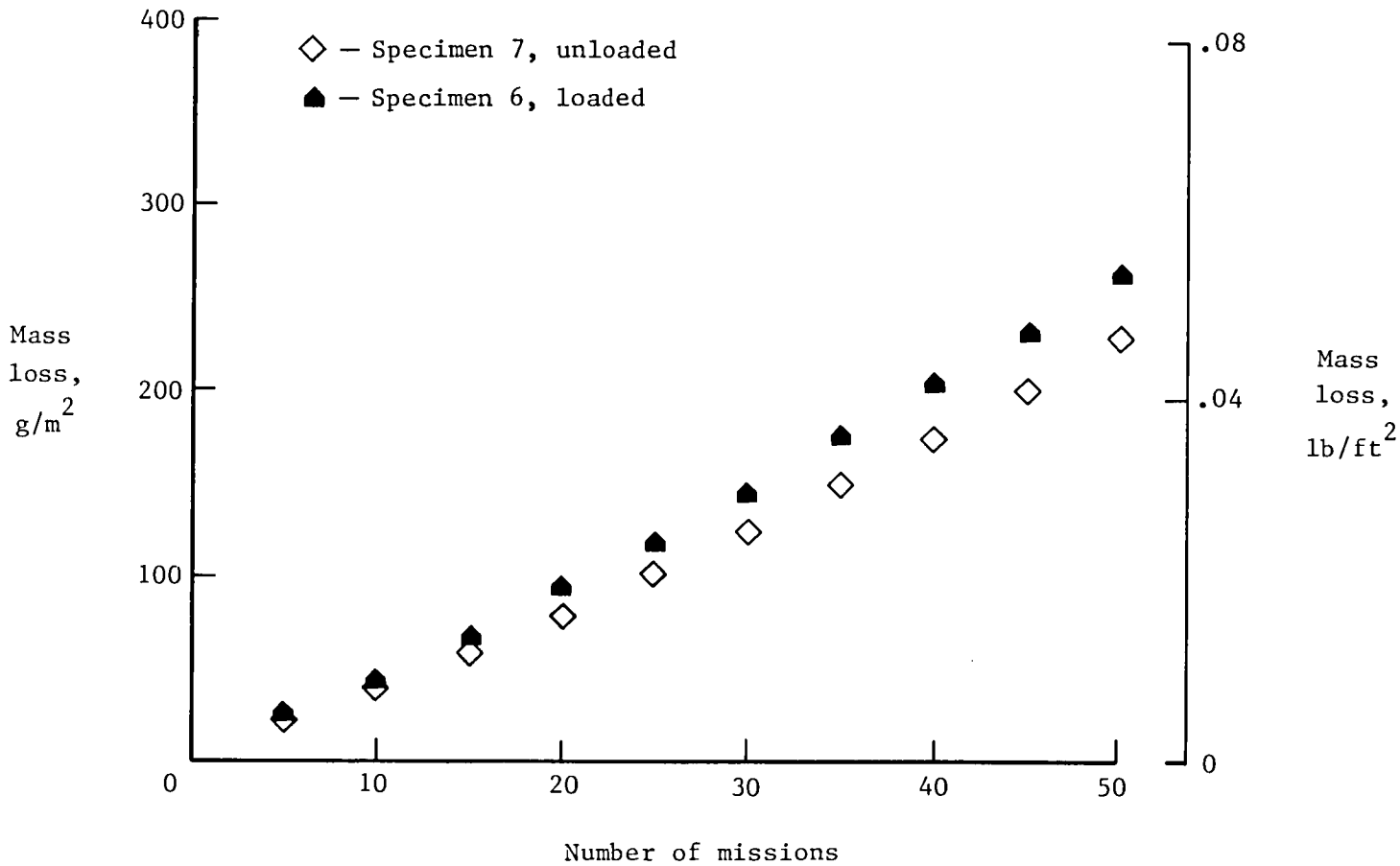

(c) Test series III.

Figure 8.- Continued.

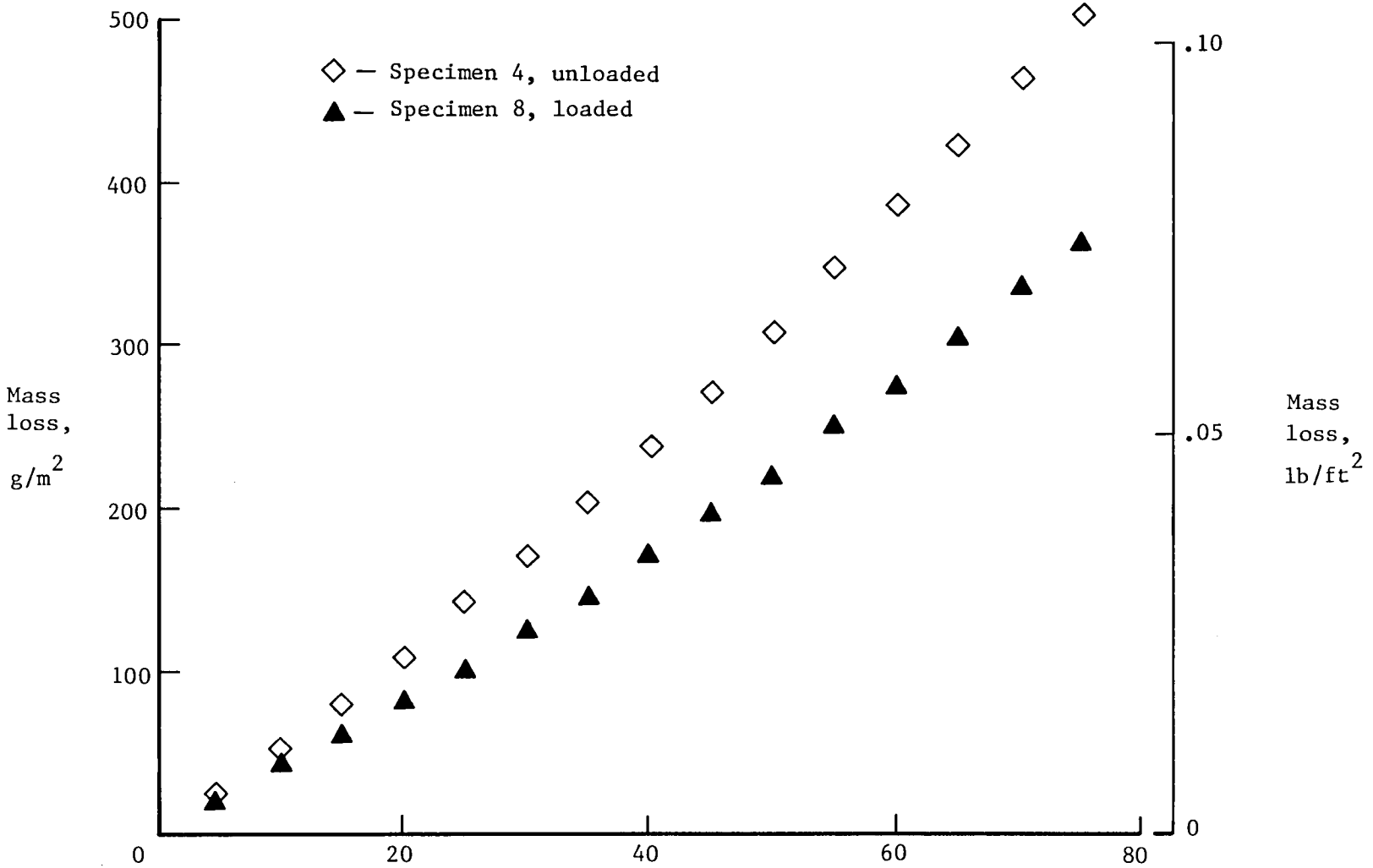

(d) Test Series IV.

Figure 8.- Concluded.

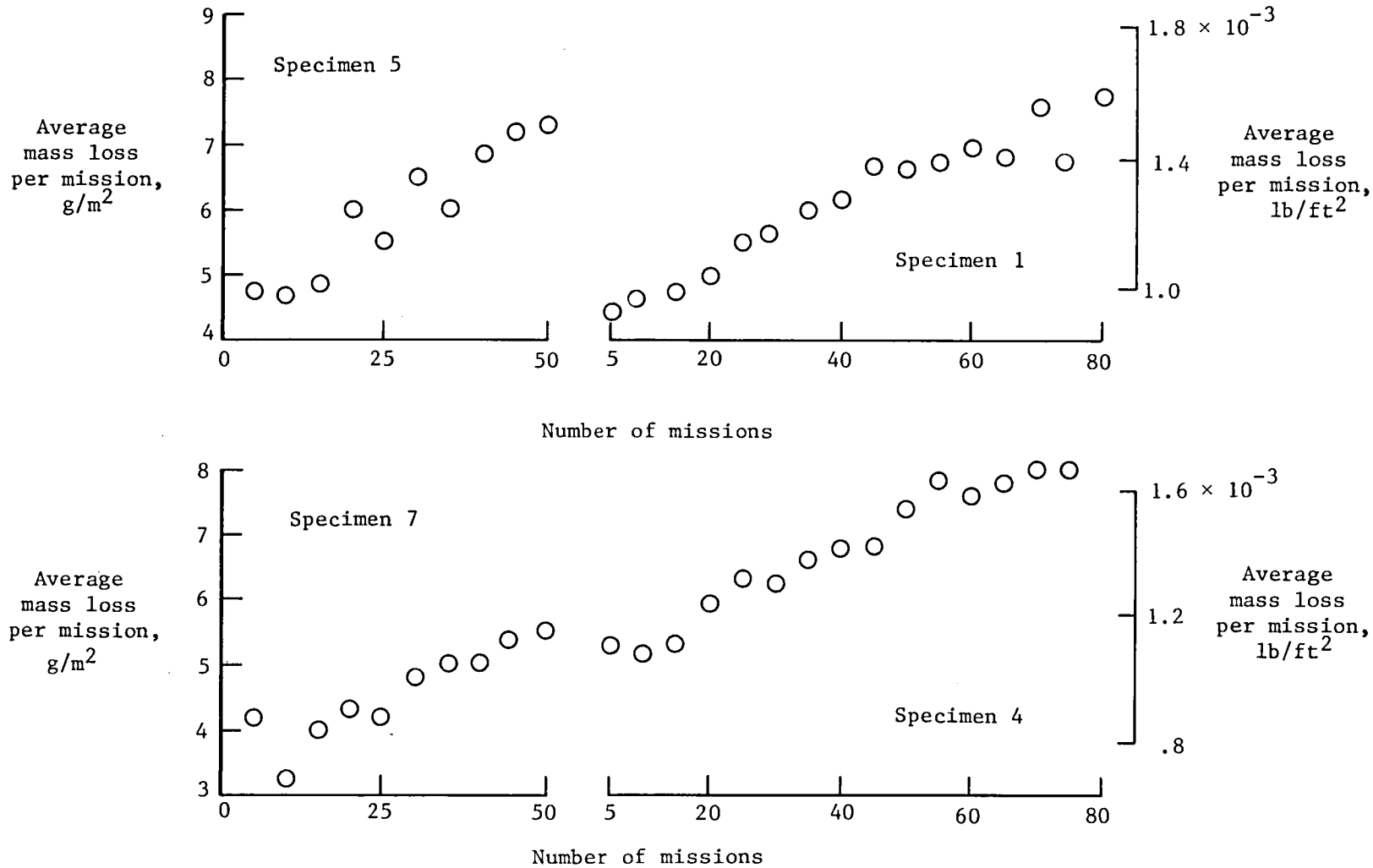

(a) Unloaded.

Figure 9.- Average mass loss per mission over five-mission increments.

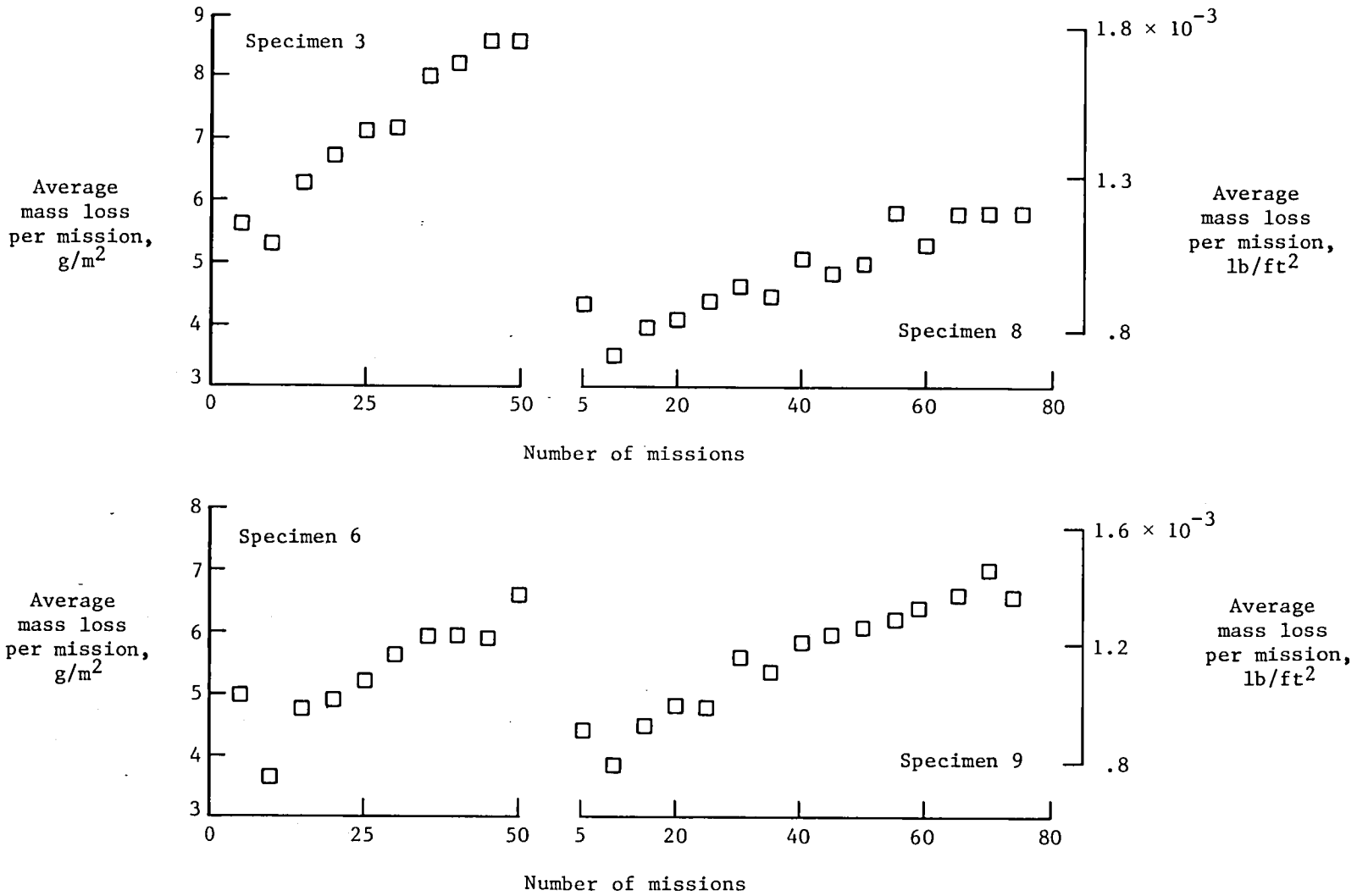

(b) Loaded.

Figure 9.- Concluded.

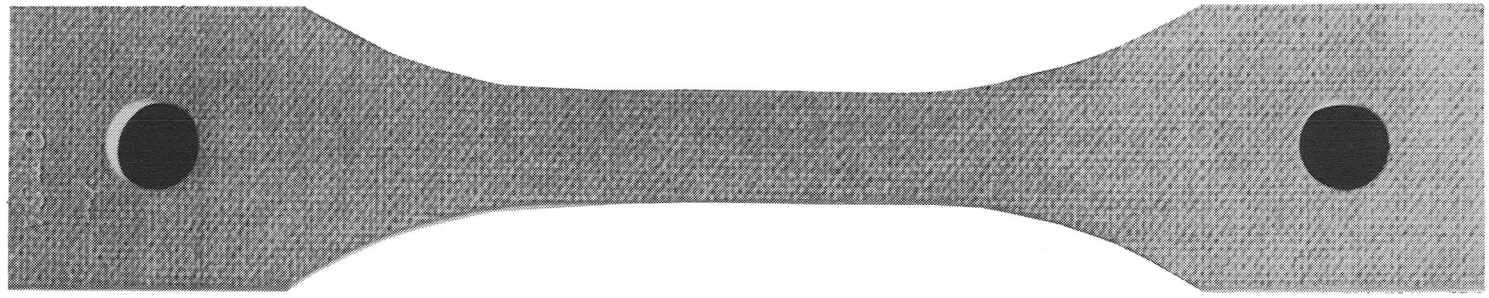

L-77-6944.1

Front

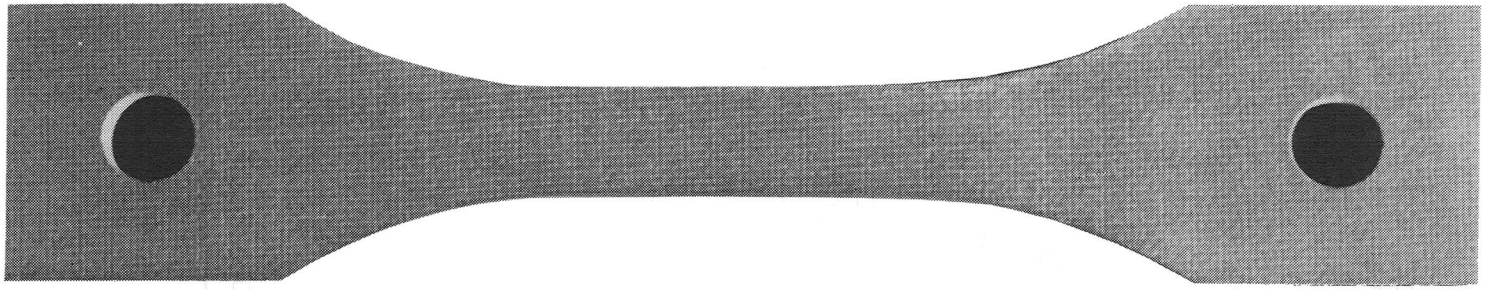

L-77-6945.1

Back

Figure 10.- Specimen 1 after 80 missions.

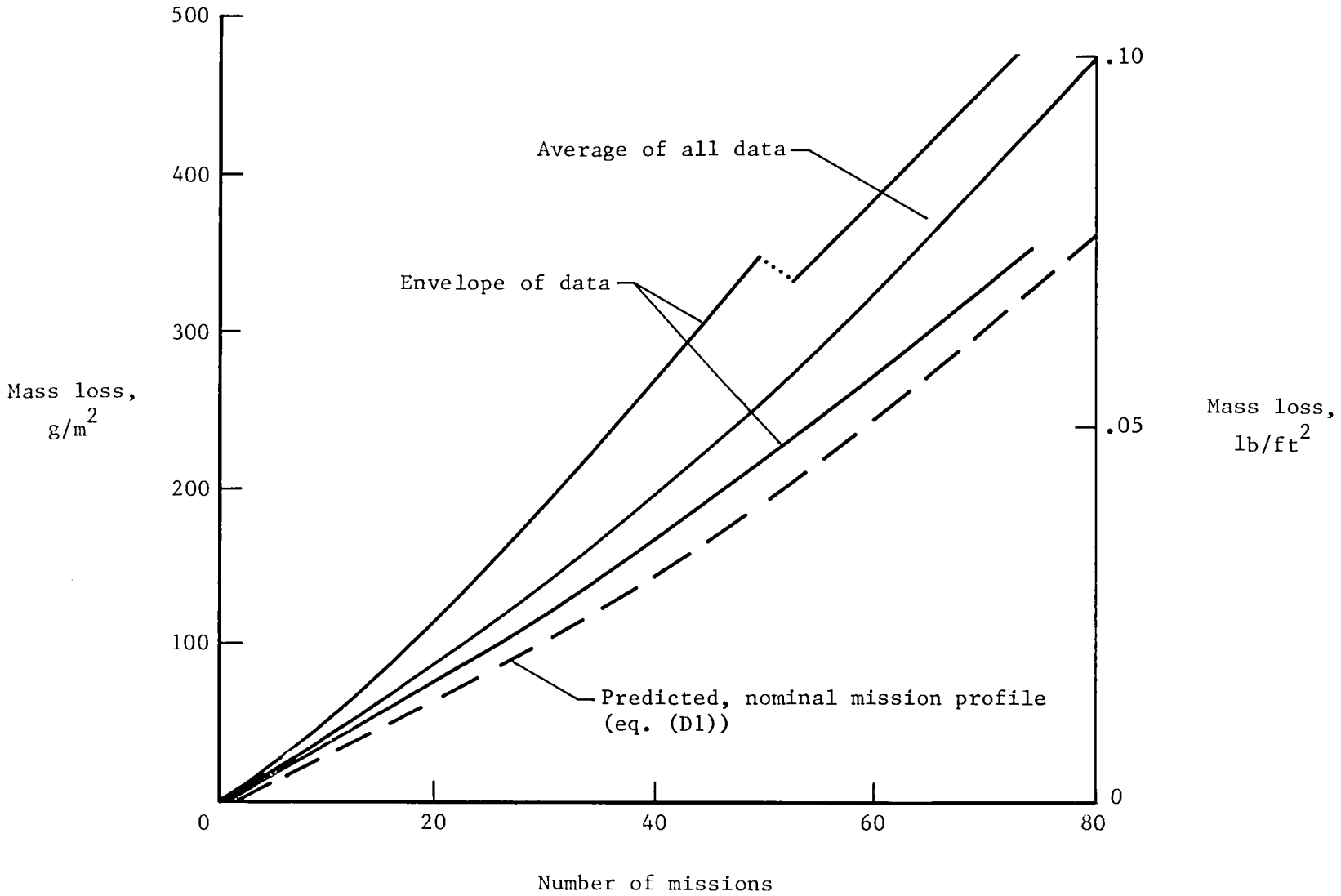

Figure 11.- Comparison of experimental mass loss with predicted mass loss using nominal mission profile.

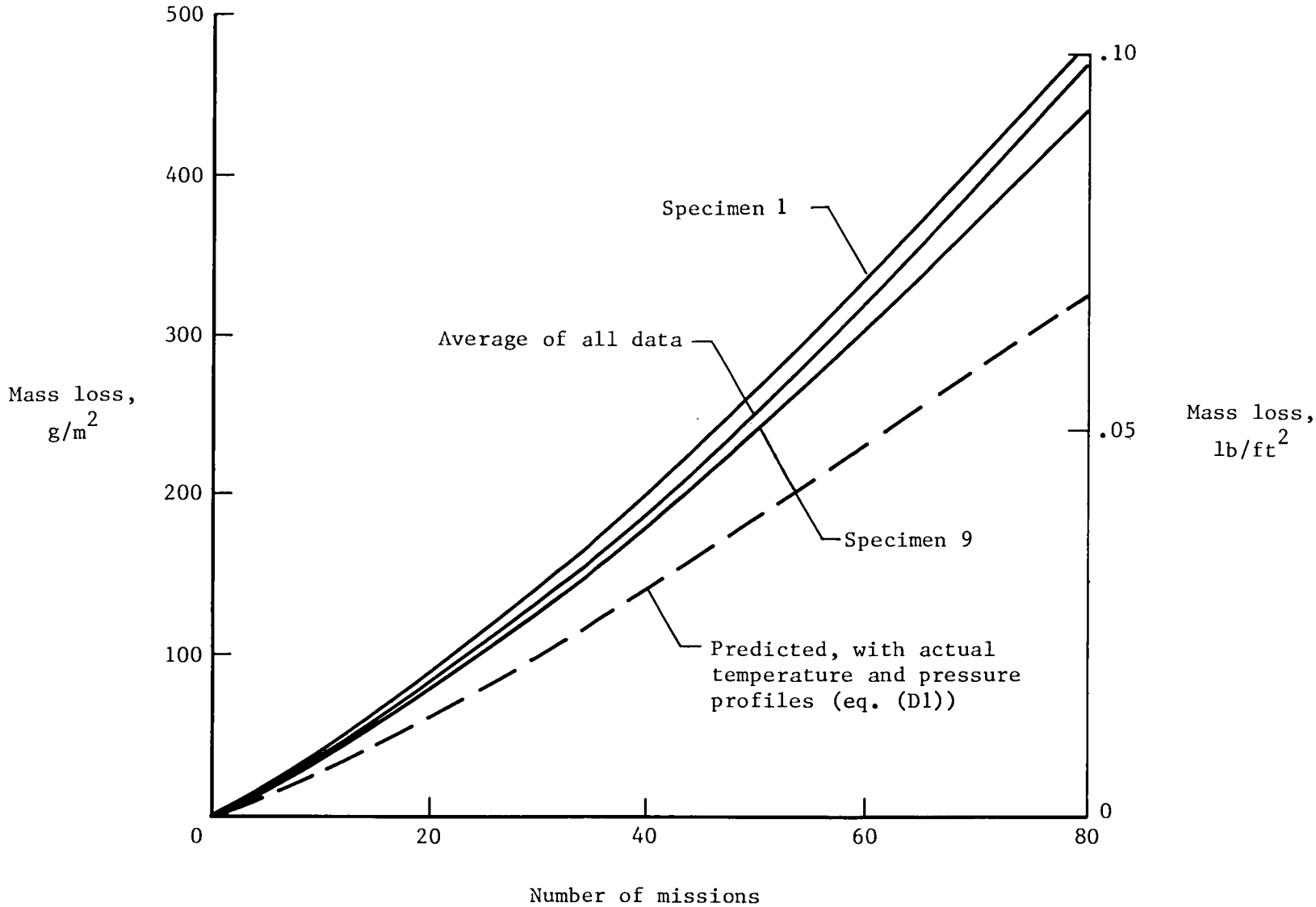

Figure 12.- Comparison of experimental mass loss with predicted mass loss using actual simulation parameters.

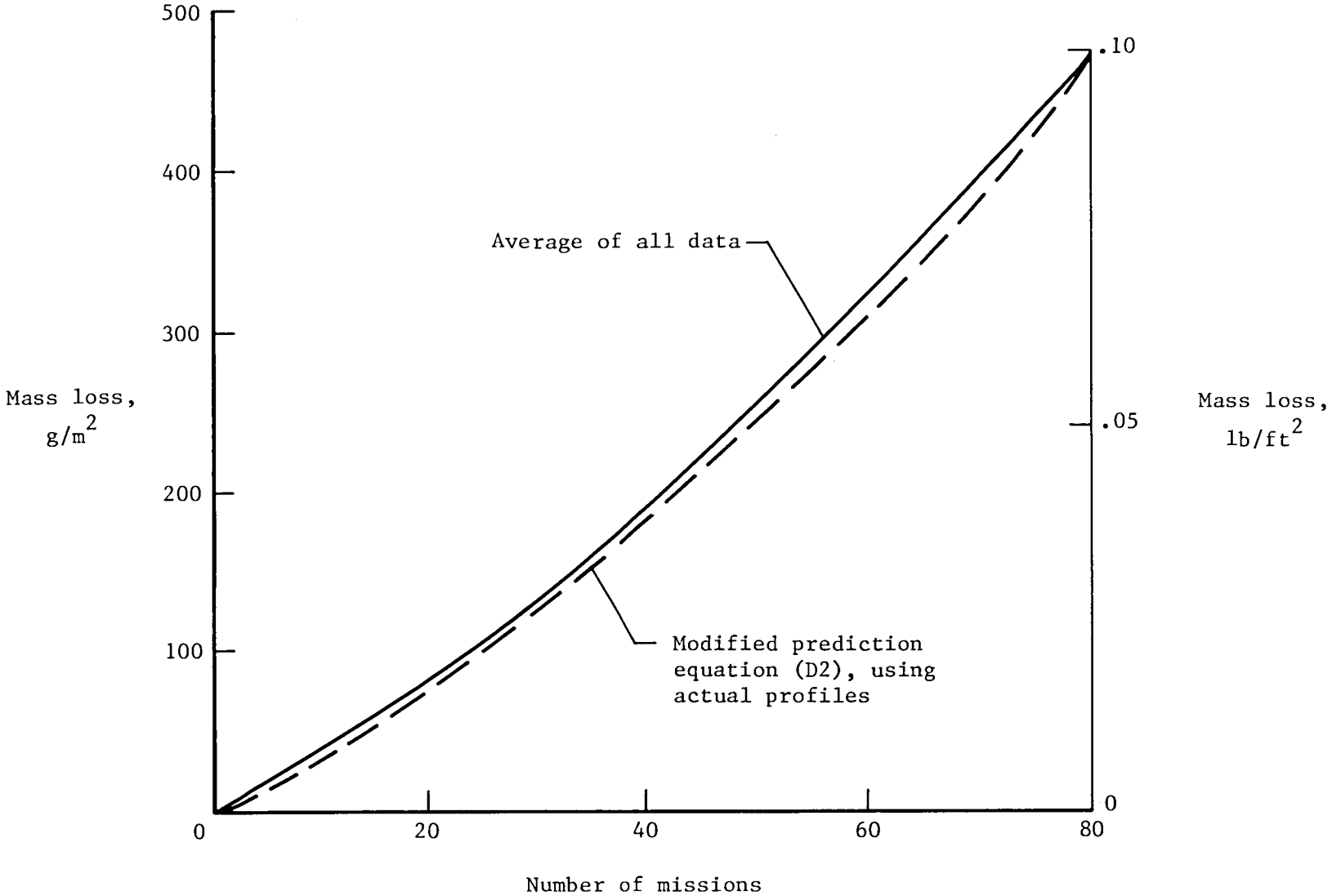

Figure 13.- Comparison of average experimental mass loss with mass loss predicted by modified equation.

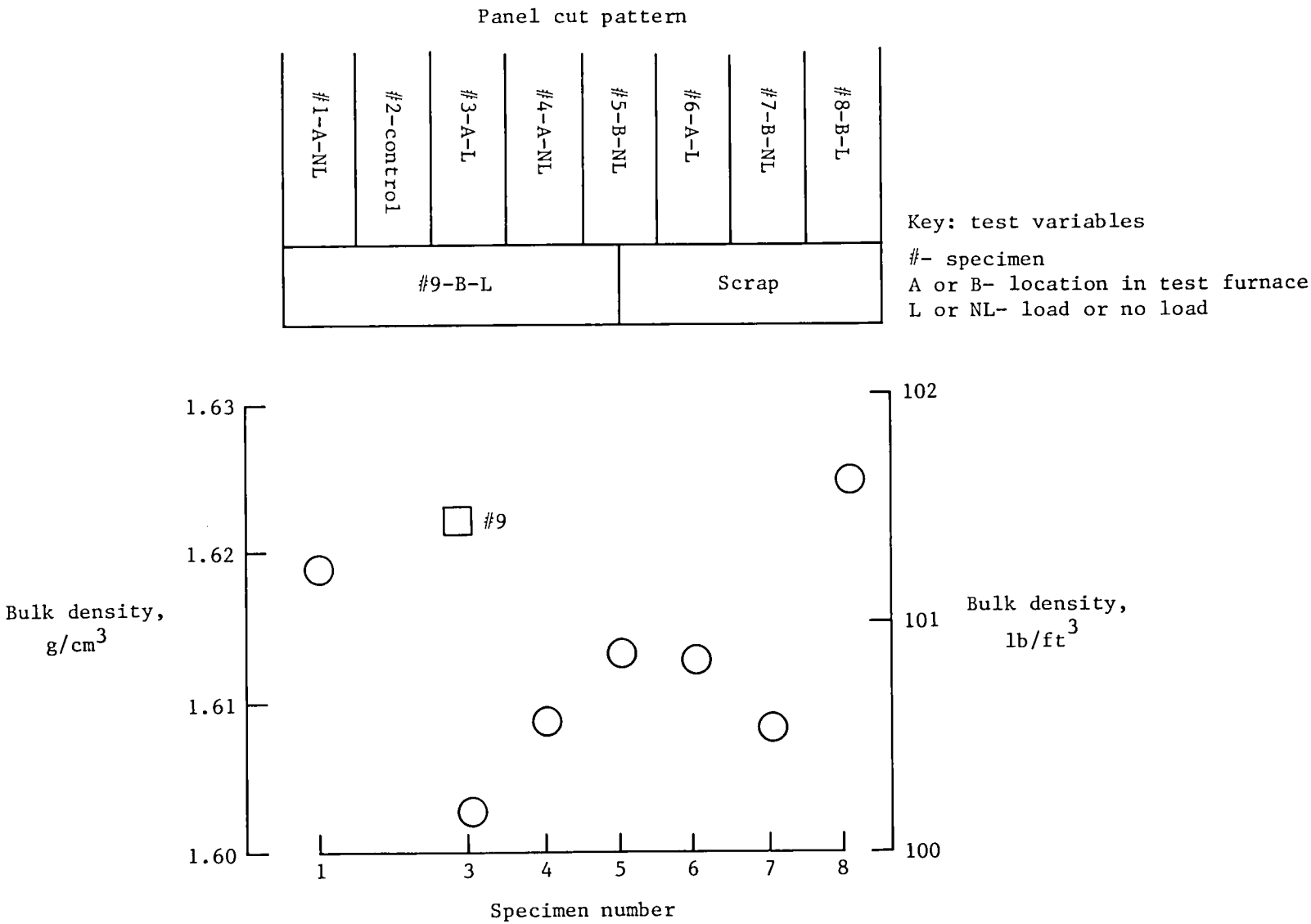

Figure 14.- Bulk density as a function of panel location.

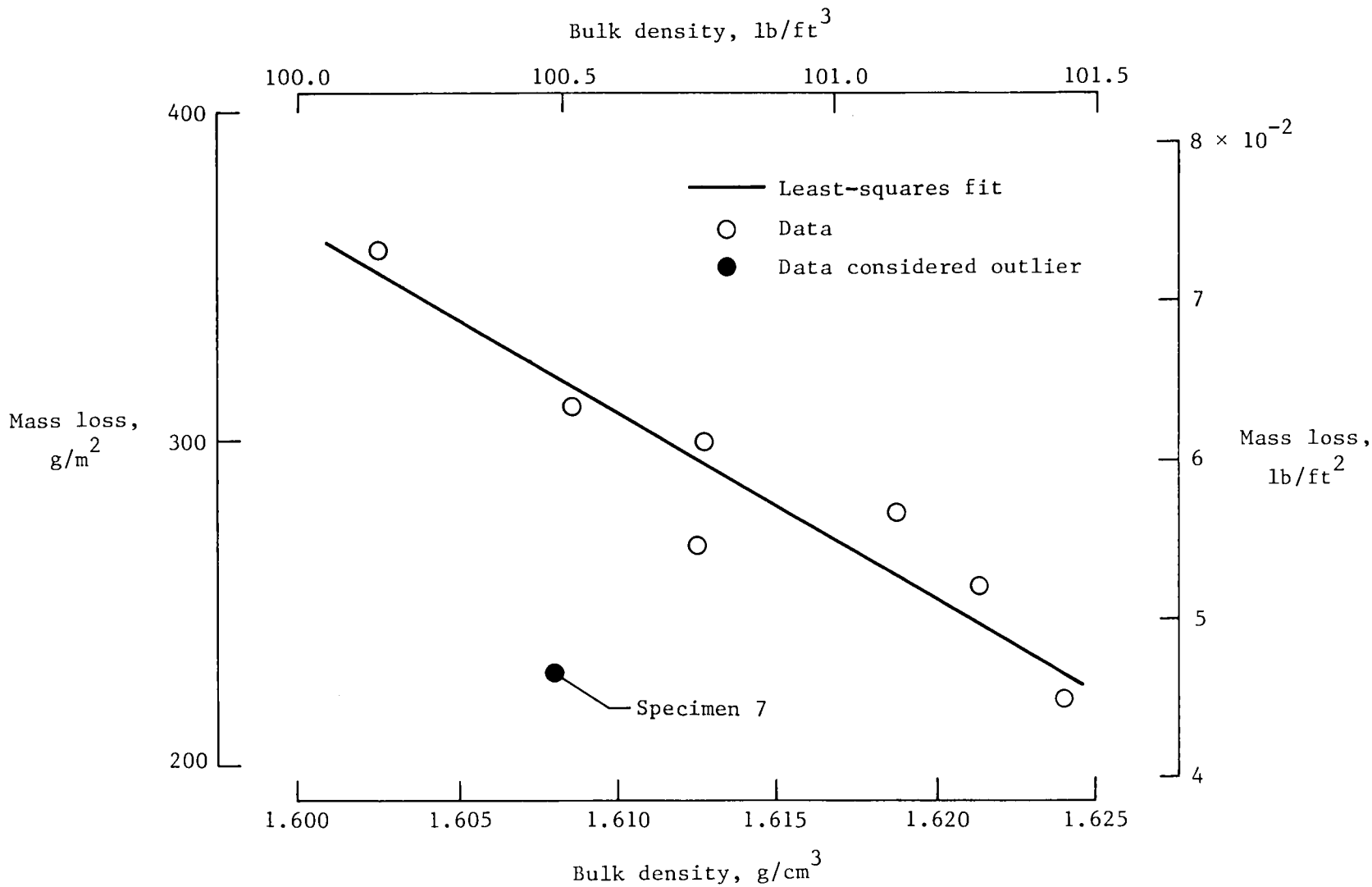

Figure 15.- Correlation of mass loss after 50 missions with initial specimen density.

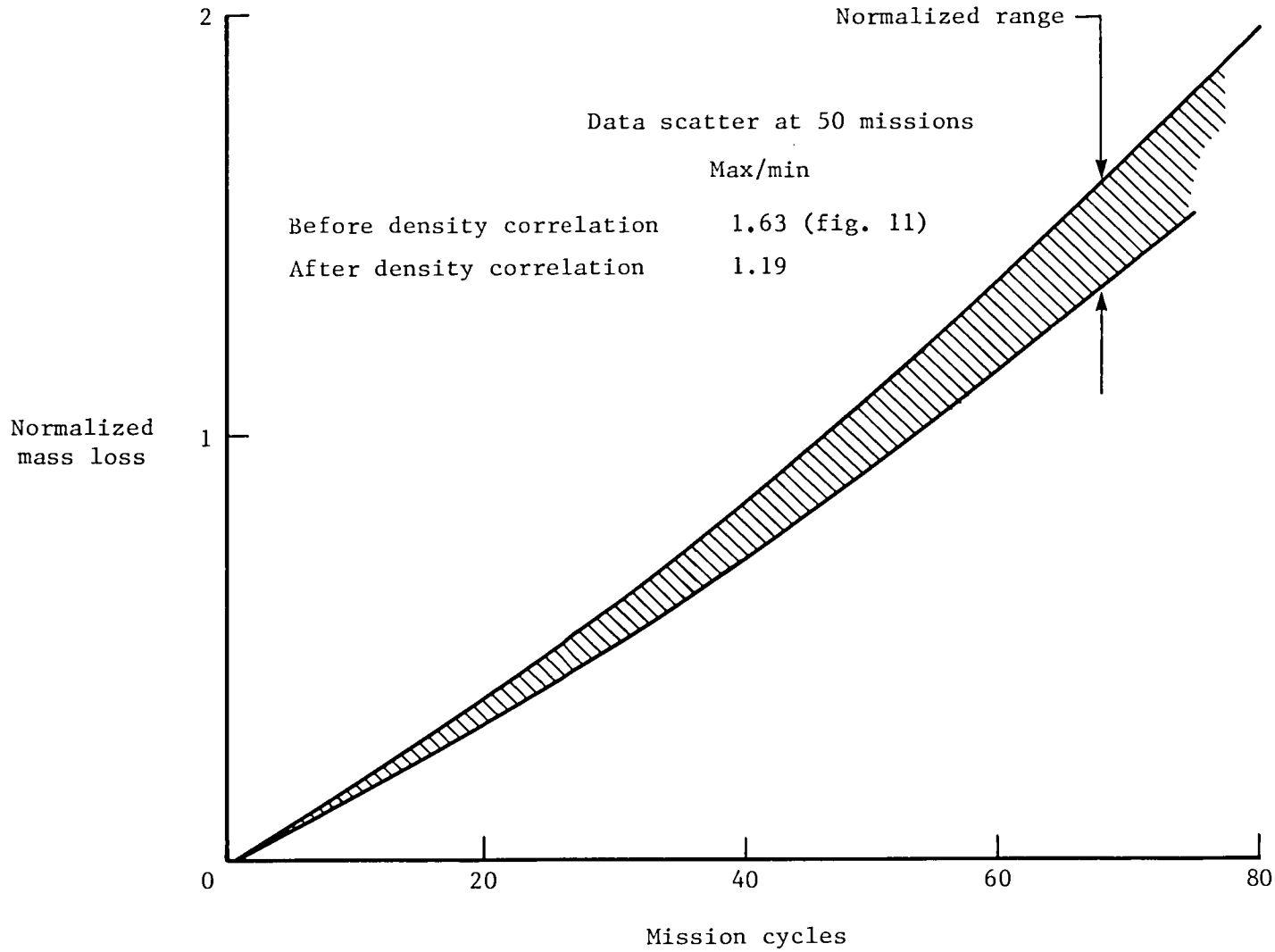

Figure 16.- Bulk density normalized mass loss.

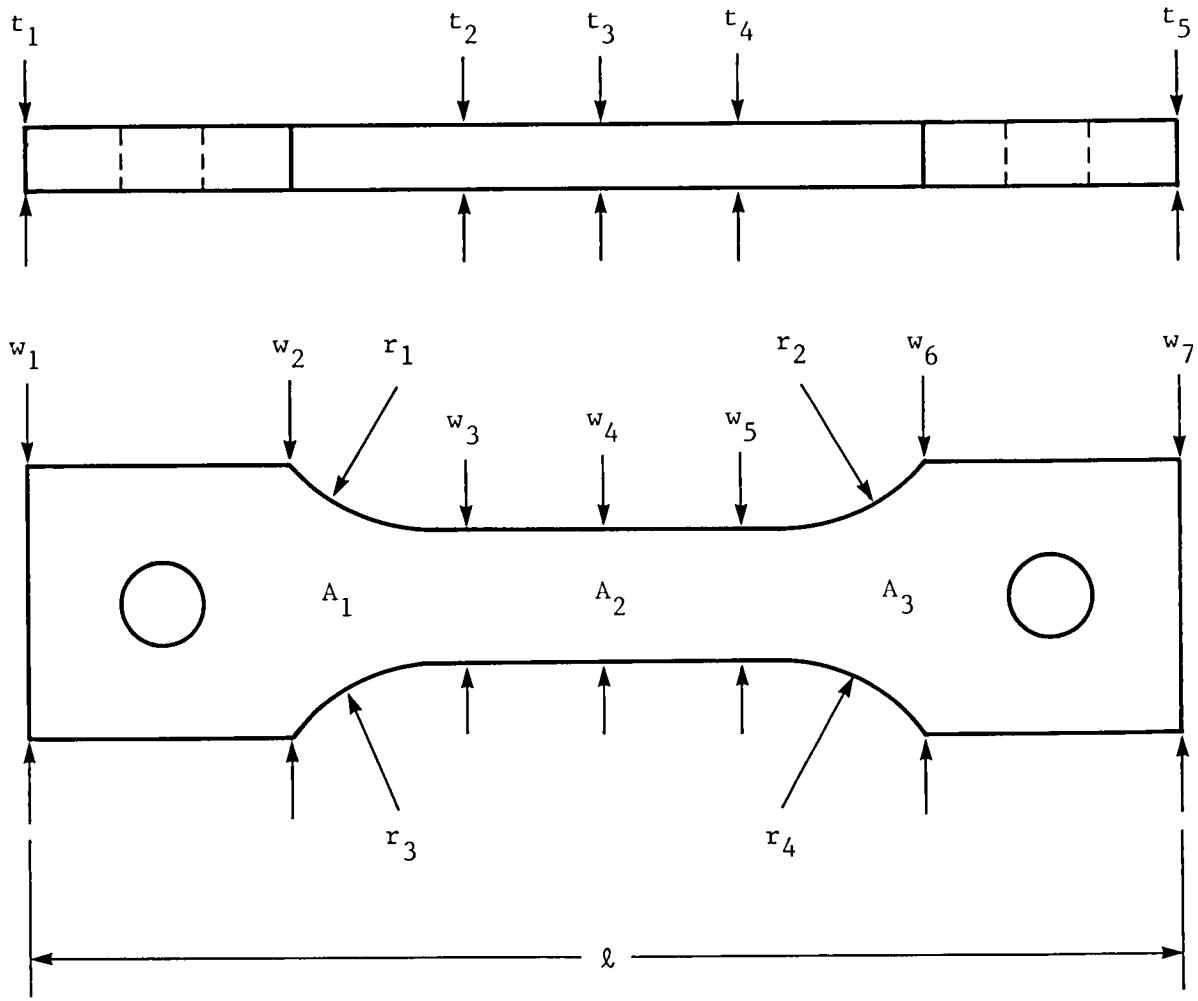

Figure 17.- Measurement locations on TEOS-coated RCC specimens.

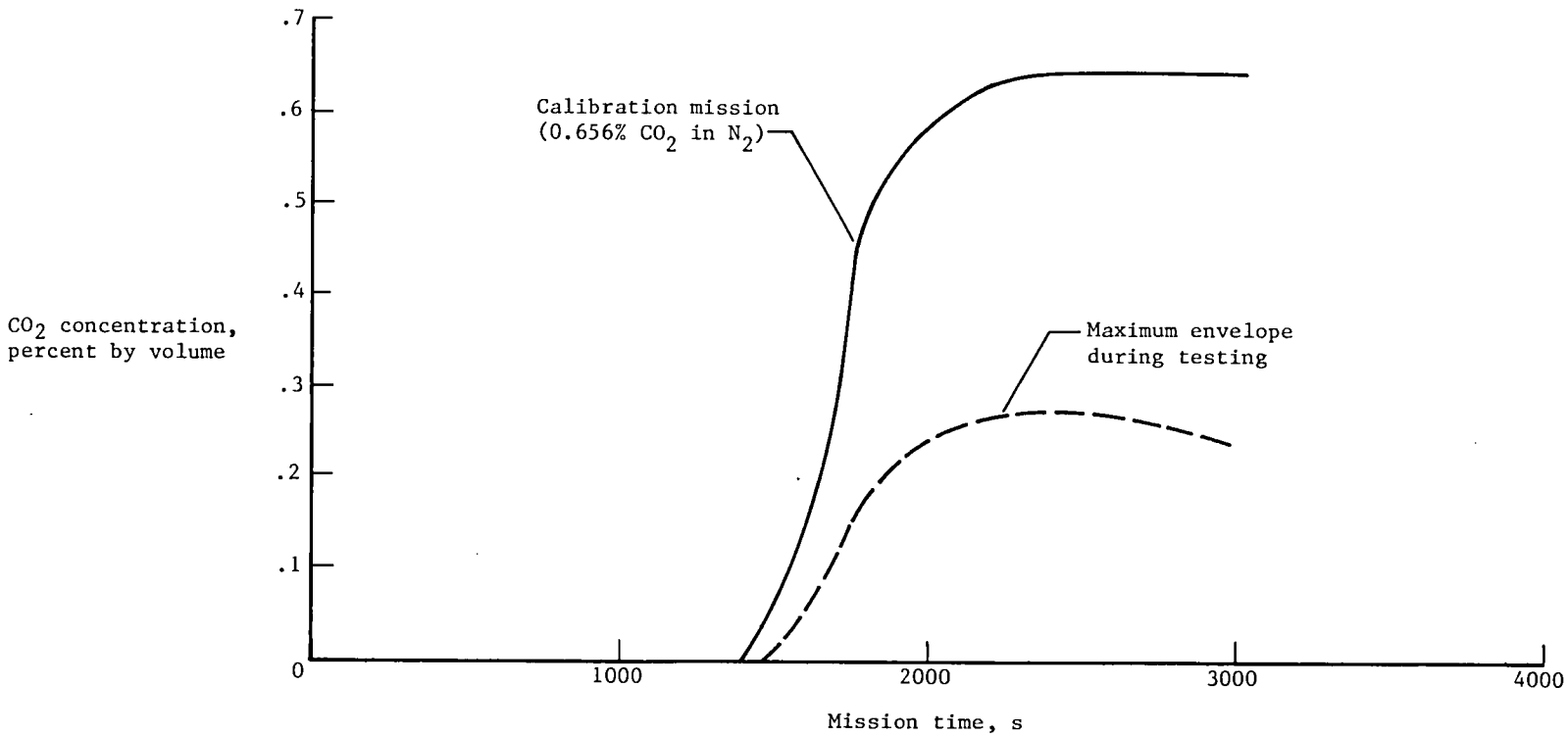

Figure 18.- Carbon dioxide concentration in test chamber effluent.

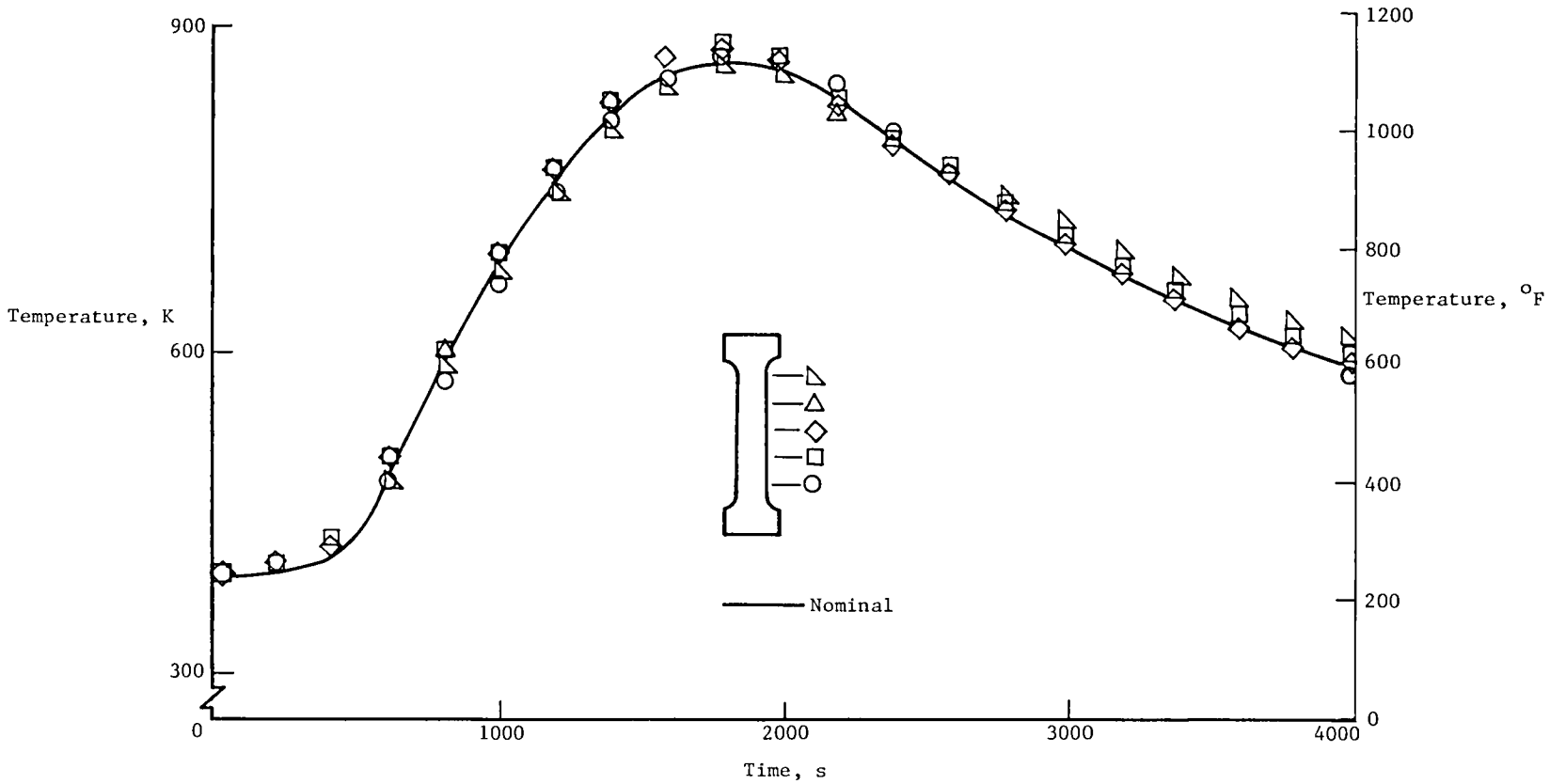

(a) Location A.

Figure 19.- Temperature profile for a typical calibration run.

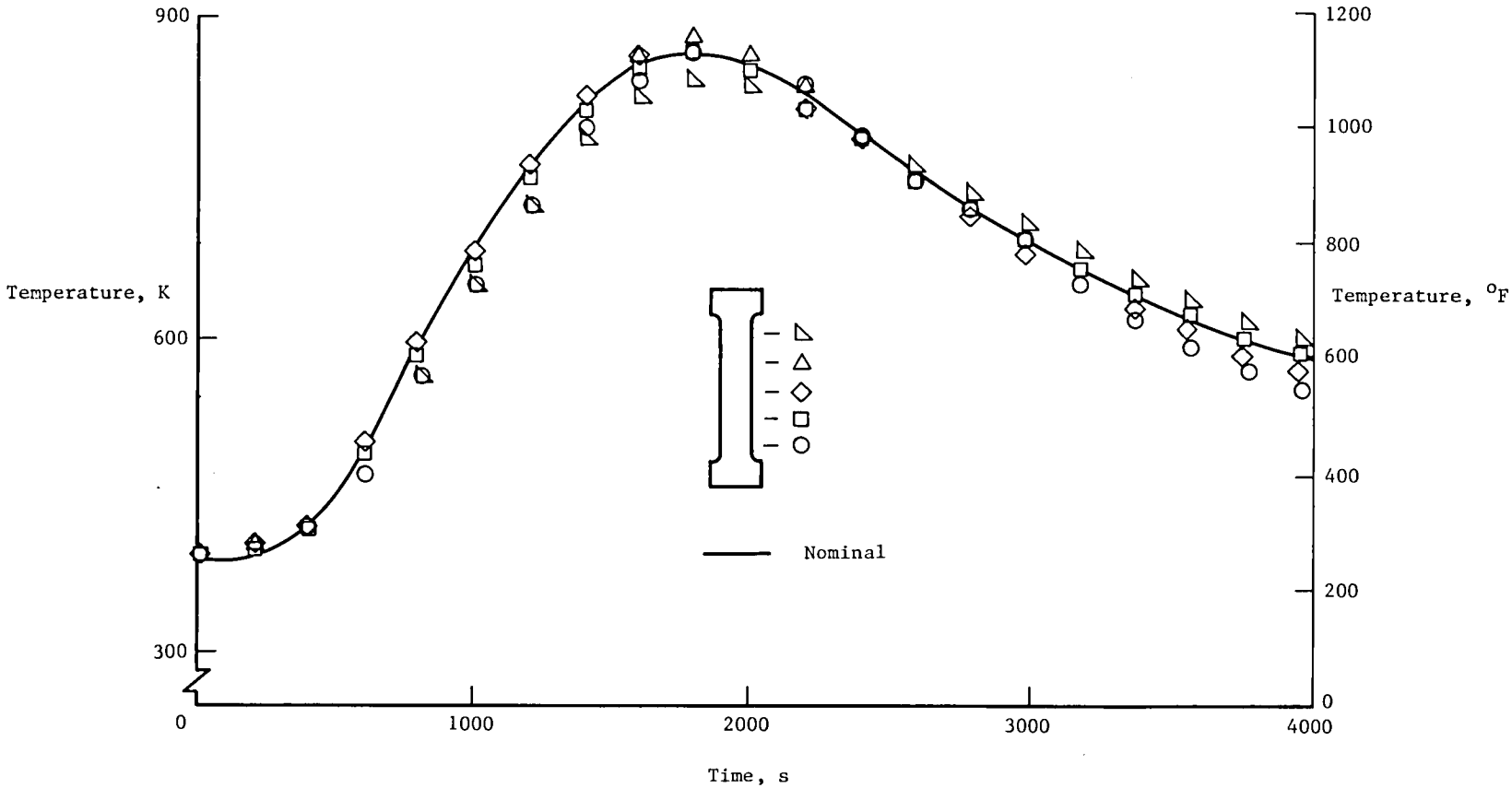

(b) Location B.

Figure 19.- Concluded.

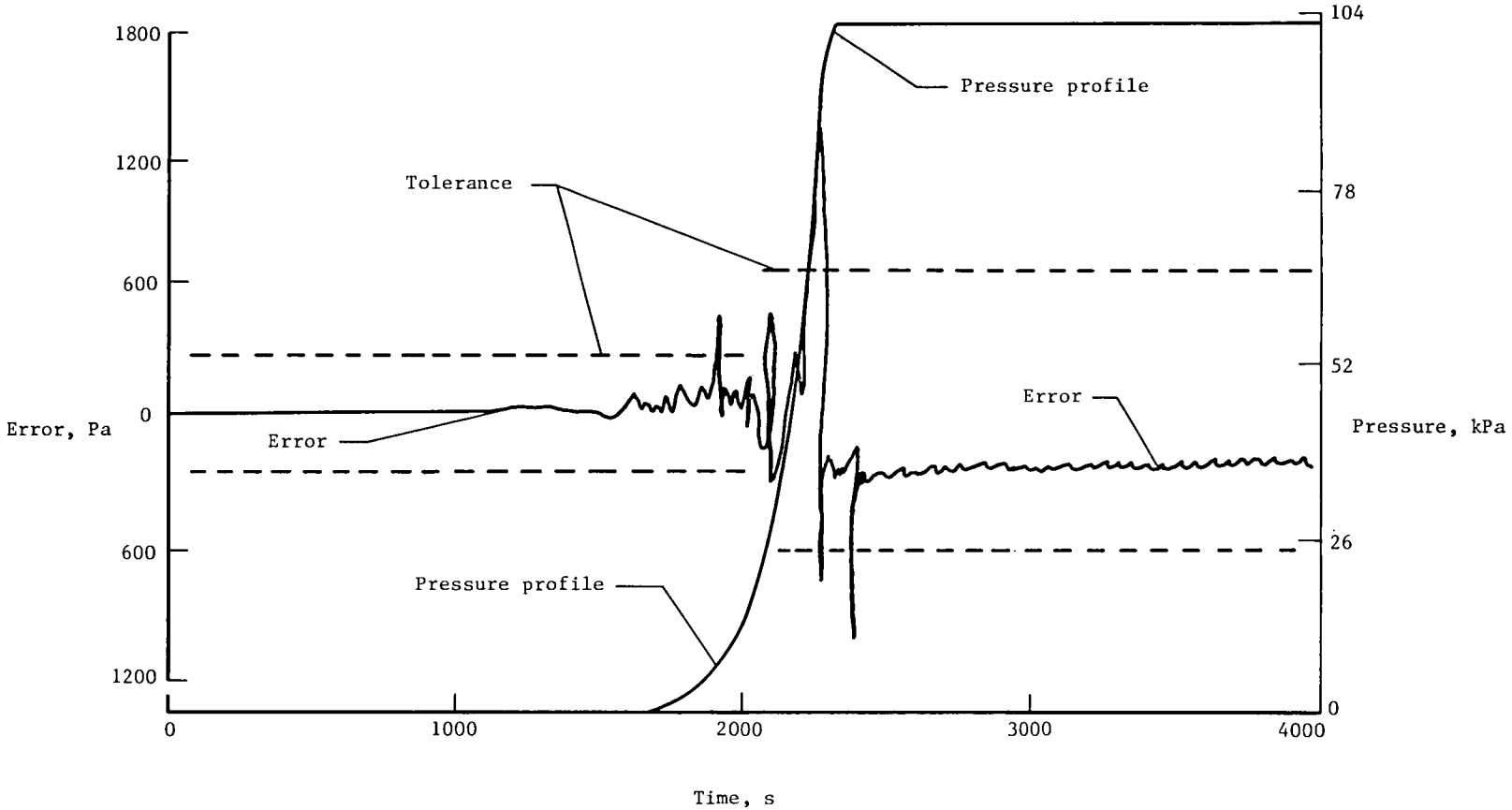

Figure 20.- Error in pressure as a function of time and pressure.

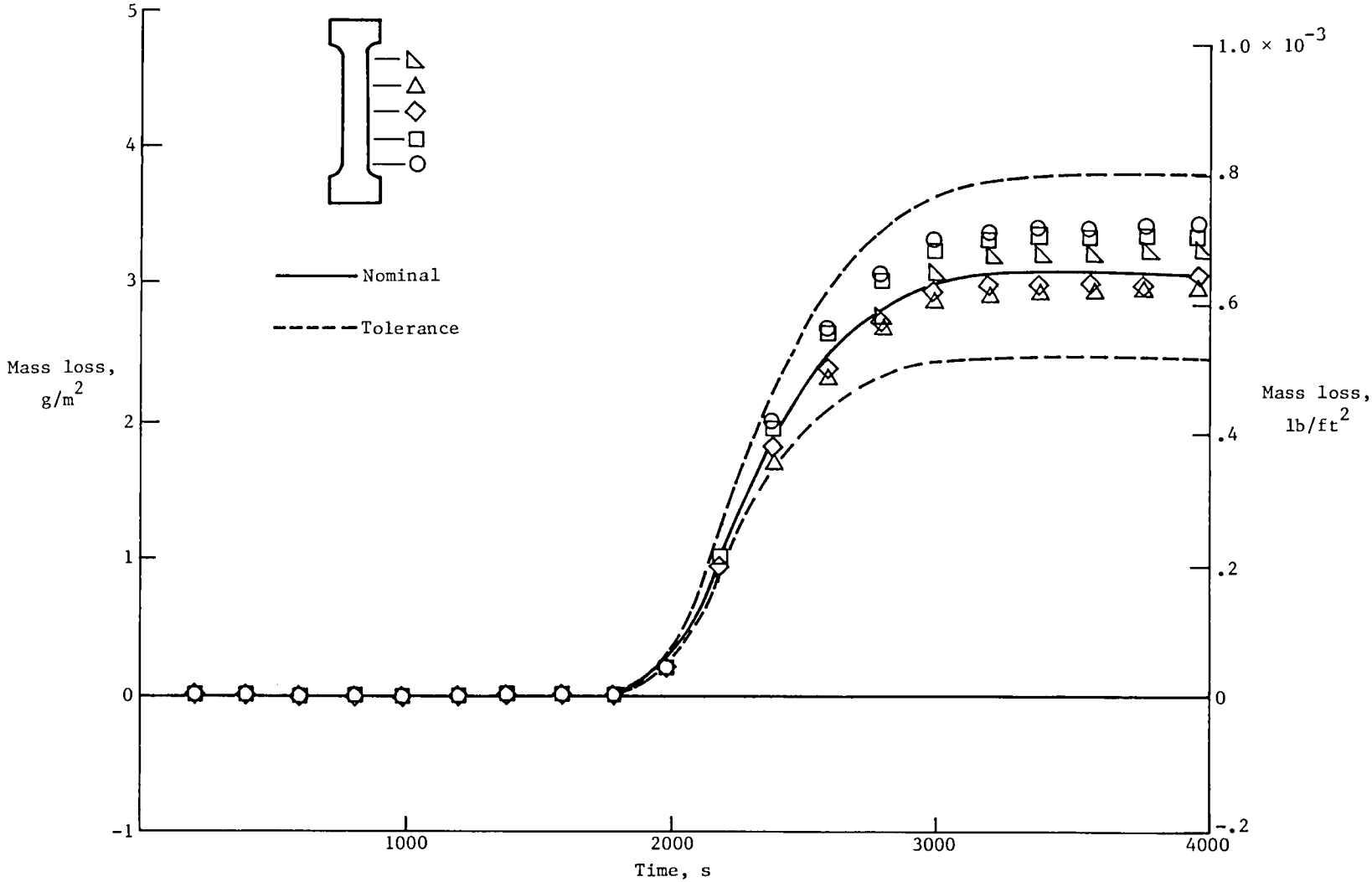

(a) Location A.

Figure 21.- Calculated mass loss for typical calibration run using measured specimen temperatures and chamber pressure.

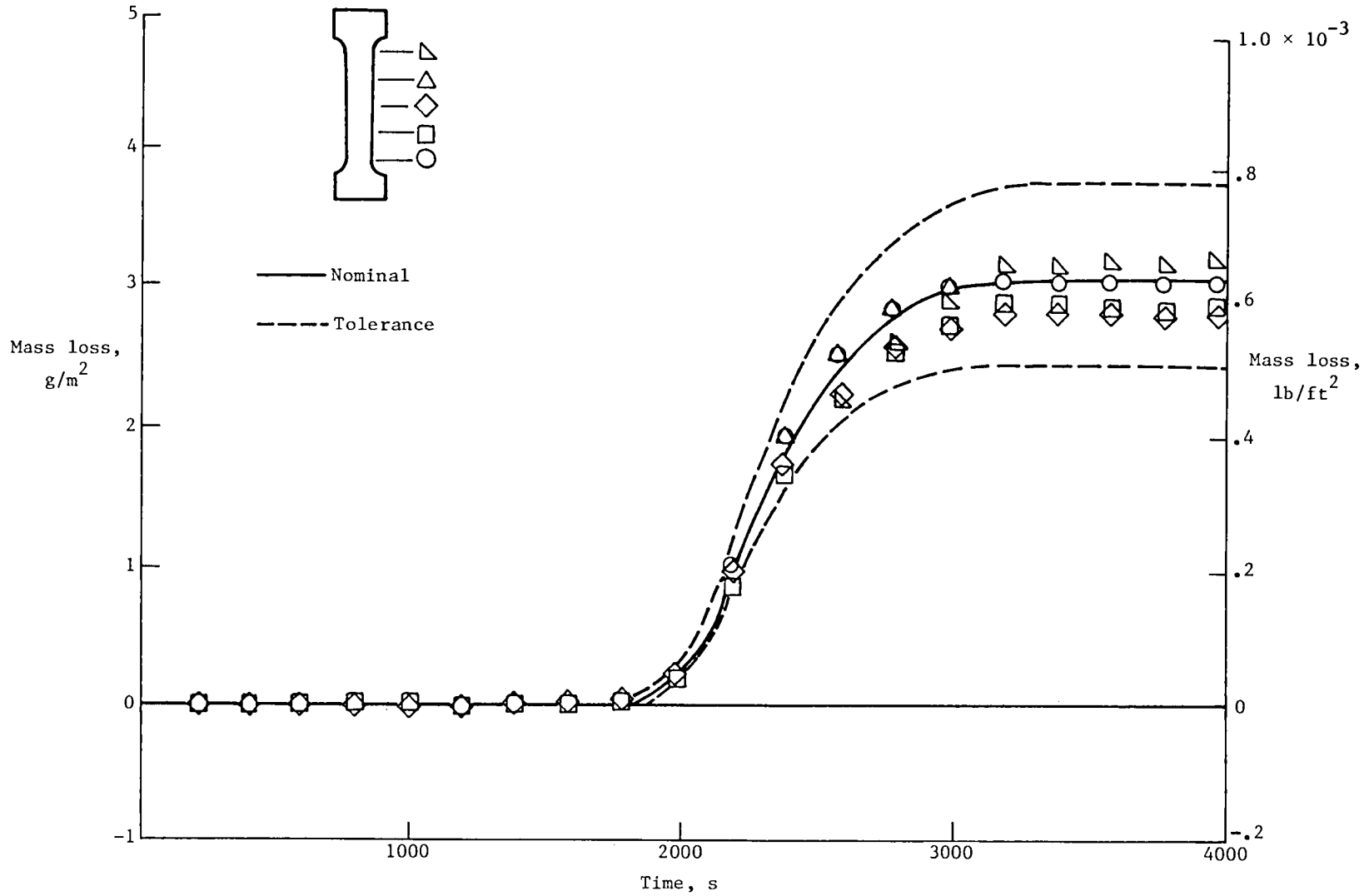

(b) Location B.

Figure 21.- Concluded.

1. Report No.	2. Government Accession No.	3. Recipient's Catalog No.
NASA TM-81799		

4. Title and Subtitle	5. Report Date
MASS LOSS OF A TEOS-COATED, REINFORCED CARBON-CARBON COMPOSITE SUBJECTED TO A SIMULATED SHUTTLE ENTRY ENVIRONMENT	July 1980
	6. Performing Organization Code

7. Author(s)	8. Performing Organization Report No.
C. W. Stroud and Donald R. Rummler	L-13400
	10. Work Unit No.
	506-53-33-01

9. Performing Organization Name and Address	11. Contract or Grant No.
NASA Langley Research Center Hampton, VA 23665	
	13. Type of Report and Period Covered
	Technical Memorandum

12. Sponsoring Agency Name and Address	14. Sponsoring Agency Code
National Aeronautics and Space Administration Washington, DC 20546	

15. Supplementary Notes

16. Abstract

Coated, reinforced carbon-carbon (RCC) is used for the leading edges of the Space Shuttle. The mass-loss characteristics of RCC specimens coated with tetraethyl orthosilicate (TEOS) were determined for conditions which simulated the environment expected at the lug attachment area of the leading edge. Mission simulation included simultaneous application of load, temperature, and oxygen partial pressure. Maximum specimen temperature was 900 K (1160° F). Specimens were exposed for up to 80 simulated missions. Stress levels up to 6.8 MPa (980 psi) did not significantly affect the mass-loss characteristics of the TEOS-coated RCC material. Mass loss was correlated with the bulk density of the specimens.

17. Key Words (Suggested by Author(s))	18. Distribution Statement
Mass loss Tetraethyl orthosilicate (TEOS) Oxidation Reinforced carbon-carbon composite (RCC)	Unclassified - Unlimited Subject Category 24

19. Security Classif. (of this report)	20. Security Classif. (of this page)	21. No. of Pages	22. Price
Unclassified	Unclassified	59	A04

For sale by the National Technical Information Service, Springfield, Virginia 22161

NASA-Langley, 1980

National Aeronautics and
Space Administration

Washington, D.C.
20546

Official Business
Penalty for Private Use, $300

THIRD-CLASS BULK RATE

Postage and Fees Paid
National Aeronautics and
Space Administration
NASA-451

NASA

POSTMASTER: If Undeliverable (Section 158 Postal Manual) Do Not Return